

Accepted Manuscript

The Little Ice Age and human-environmental interactions in the Central Balkans:
Insights from a new Serbian paleorecord

Charuta Kulkarni, Dorothy, M. Peteet, Rebecca Boger



PII: S1040-6182(17)31238-7

DOI: [10.1016/j.quaint.2018.04.035](https://doi.org/10.1016/j.quaint.2018.04.035)

Reference: JQI 7396

To appear in: *Quaternary International*

Received Date: 6 September 2017

Revised Date: 4 April 2018

Accepted Date: 23 April 2018

Please cite this article as: Kulkarni, C., Peteet, D., M., Boger, R., The Little Ice Age and human-environmental interactions in the Central Balkans: Insights from a new Serbian paleorecord, *Quaternary International* (2018), doi: 10.1016/j.quaint.2018.04.035.

This is a PDF file of an unedited manuscript that has been accepted for publication. As a service to our customers we are providing this early version of the manuscript. The manuscript will undergo copyediting, typesetting, and review of the resulting proof before it is published in its final form. Please note that during the production process errors may be discovered which could affect the content, and all legal disclaimers that apply to the journal pertain.

1 **The Little Ice Age and human-environmental interactions in the Central Balkans: insights**
2 **from a new Serbian paleorecord**

3 Kulkarni, Charuta,^{1*} Peteet, Dorothy, M.^{2,3} and Rebecca Boger^{1,4}

4 ¹Department of Earth and Environmental Sciences, The Graduate Center of CUNY, 365 Fifth
5 Avenue, New York, NY 10016, USA.

6 ²NASA/Goddard Institute for Space Studies, 2880 Broadway, New York, NY 10025, USA.

7 ³Lamont-Doherty Earth Observatory of Columbia University, 61 Rte. 9W, Palisades, NY 10964,
8 USA.

9 ⁴Department of Earth and Environmental Sciences, Brooklyn College of CUNY, 2900 Bedford
10 Avenue, Brooklyn, NY 11210.

11 *Author for correspondence: e-mail: ckulkarni@gradcenter.cuny.edu

12 Abstract

13 This paper presents a 600-year well-dated, high-resolution Central Balkan paleo-record including
14 the Little Ice Age (LIA; 1450-1850 CE). Utilizing pollen-based REVEALS modelling estimates,
15 geochemical indicators, rarefaction analyses and the AMS ¹⁴C-based Bacon age model, this first-
16 hand record from the Sava Basin reveals the transformation of the Central Balkan landscape
17 involving linkages between changing climatic and socio-political regimes. The pre-LIA interval
18 (1370-1418 CE) in the Sava Region reveals a wooded steppe and increased cultivation under
19 warmer/stable climatic and socio-political conditions. In contrast, the LIA interval in the region
20 is expressed through continuous transitions between forest and grassland, extensive land erosion
21 and stressed agriculture, potentially as a collective artifact of the climatic variability and human
22 impact associated with socio-political stressors of the time. The post-LIA/Industrial Era interval
23 (1850-2012 CE) in the Sava Region shows an overall increase in woodland as well as agriculture
24 following the exit of the Ottomans. However, increased population pressures and the subsequent
25 onset of the Industrial Revolution as well as increased trade led to intense deforestation
26 throughout the 20th Century, which continued during the Socialist period.

27

28 Keywords

29 The Common Era; Little Ice Age climate variability; Pollen-based REVEALS modelling,
30 Charcoal analysis; Geochemistry; Societal impacts of climate change

31 **1. Introduction**

32 Continuing global climate change and its potential threats to ecosystems and humans present a
33 substantial challenge to modern civilizations (Cook et al., 2015). In many regions, increasing
34 temperatures and changing precipitation patterns are altering hydrological and ecological
35 systems thereby influencing water resources, agricultural productivity, human health, and even
36 social conflicts. Furthermore, the degree and intensity of these impacts is likely to increase in the
37 future as human-induced environmental changes continue their substantial imprint on a
38 background of natural climatic variability (Bradley and Jones, 1993a; Buntgen et al., 2011). The
39 Common Era i.e. the past 2000 years reveals examples where human influences have increased
40 to the extent that they became capable of strengthening/attenuating the impacts of climatic
41 processes (e.g. intensification/weakening of evaporation; Reale and Shukla, 2000). To envision
42 the vulnerability and sustainability of future complex socio-environmental systems, it is
43 important to improve our understanding of the nature of critical climatic episodes in the
44 Common Era (e.g. Little Ice Age (LIA), Medieval Climate Anomaly (MCA)), associated societal
45 responses and environmental changes for elucidating details of climate-human-ecosystem
46 interactions (Mercuri and Sadori, 2014; PAGES Hydro2k Consortium, 2017).

47 This multi-proxy study explores the central Balkan vegetation and landscape change in
48 the context of climatic variability and human impact over the past 600 years. This time interval
49 includes the late-14th and early-15th centuries (a transitional period between MCA and LIA;
50 Masson-Delmotte et al., 2013), the full extent of the LIA (1450–1850 CE; Bradley and Jones,
51 1993, 1992; Lamb, 1965; Mann, 2002), and the post-LIA/Industrial Era. Among these, the LIA is
52 of particular interest as its nature and magnitude varies across Europe (Bradley and Jones,
53 1993b; Mann et al., 2009; Ljungqvist, 2010). Overall, the LIA is identified as a time when

54 Northern Hemisphere annual temperatures were cooler and winters were significantly colder
55 with increased winter precipitation (Bradley and Jones, 1993b; Jones et al., 1998; Mann et al.,
56 1999). However, it is argued that a standard wet-cold picture of the LIA is based on a number of
57 proxy records from northern-western parts of Europe while the LIA in the east-south Europe
58 could be cold but drier (Luterbacher et al., 2011; Roberts et al., 2012; Cook et al., 2016). Recent
59 proxy as well as modeling datasets from the Mediterranean region highlight that the east-west
60 climate see-saw seems to have operated at the two ends of the region for the last 1100 years,
61 implying a drier eastern Mediterranean region during the LIA preceded by wetter MCA
62 conditions (Luterbacher et al., 2011; Roberts et al., 2012). While western Mediterranean
63 aridity/humidity patterns appeared consistent during the MCA/LIA periods, the pattern is less
64 clear in the eastern Mediterranean, due to unavailability of high-resolution last-millennium proxy
65 datasets (Zerefos et al., 2011; Roberts et al., 2012; Gogou et al., 2016). The Balkan Peninsula is a
66 key climatic transition zone between the western and eastern Mediterranean, and between the
67 Mediterranean and the Central European region (Qiriazi and Sala, 2000; Xoplaki et al., 2001).
68 Consequently, this new multi-centennial paleoecological record from the Sava Region – part of
69 the understudied Balkans (Fig. 1a) – and its correlation with the existing literature advances our
70 understanding of the nature and spatial variability of the LIA across the region while identifying
71 its implications and interactions with contemporary human and environmental systems.

72

73 **2. Study area**

74 **2.1 Regional setting and study site**

75 The Republic of Serbia comprises 16% of the Sava Basin (Milačić et al., 2014), its downstream
76 portion west of the Sava-Danube confluence at Belgrade. The Sava Basin is part of Pannonian

77 Plains (Fig. 1b), comprising Quaternary alluvial floodplains with gentle slopes and little relief,
78 which are truncated by the Fruska Gora Mountains in the north and Dinaric massifs in the south
79 (Cvetkovic et al., 2007; Toljić et al., 2013). The sediment record in this study is derived from an
80 oxbow lake “Zivaca” of the Sava River (44°44'7.41"N, 20°10'57.21"E, 65 m a.s.l., Fig. 1b-c) The
81 total area of the oxbow is ~1.27 km² with a perimeter of ~9 km. It is located 24 km west of
82 Belgrade city (Fig. 1b). The site is protected from large-scale flooding of the Sava main channel
83 through an artificial flood levee structure, however, it is partially waterlogged by groundwater
84 during the spring period (Kitnaes et al., 2009).

85 **2.2 Climate**

86 The Sava Region (overall, Serbia) experiences a continental climatic regime with cold, relatively
87 dry winters and warm, humid summers. The mean annual air temperature for lower altitudes
88 (<300 m) is 11°C with a maximum temperatures range of 37-42°C in July (RHMSS, 2015). The
89 region has a continental precipitation pattern with more rainfall in the warmer part of the year;
90 June is the wettest month receiving 12 to 13% of total (Sekulić et al., 2012). The annual
91 precipitation along the lower elevations is 600-800 mm/year varying with elevation and exposure
92 (RHMSS, 2015). Snow cover is characteristic from November to March with January as the
93 snowiest month.

94 **2.3 Regional and local vegetation**

95 Horvat et al. (1974) describes the vegetation in the study area as part of the Pannonian forest-
96 steppe zone, characterized by stands of deciduous sessile oak and maple communities, e.g.
97 *Quercus pubescens-petraea* Br.-B1.1931 and *Acer tataricum* Zol. et Jak. 1956. These
98 thermophile communities are accompanied by mesophilous taxa including *Carpinus betulus* L.
99 and *Fagus moesiacum* L. along shaded cool valleys-exposures in the lowlands (Rakonjac and

100 Nevenic, 2012). The Fruska Gora Mountains (~50 km north of the study site) comprise the
101 Central Balkanic beech forest, dominated by *Fagus sylvatica* L. along with *Q. robur-cerris* L.,
102 *Carpinus betulus* L. and *Tilia tomentosa* L. The riparian vegetation along the Sava River
103 includes *Salix alba* L., *S. amygdaloides* Andersson, *Populus nigra* L., and *Acer negundo* L. with
104 scrub populations of *Cornus sanguinea* L., *Corylus avellana* L., and occasionally *Vitis vinifera*
105 L. Regularly inundated forests especially during the spring-autumn include *Alnus glutinosa* (L.)
106 Gaertn., *Quercus robur* L., *Fraxinus angustifolia* Vahl., *U. minor* Mill. with a shrubland of *Acer*
107 *campestre* L., *Salix cinerea* L., and *Sambucus nigra* L. The stratum of herbaceous plants
108 comprise Amaranthaceae family, Asteraceae family (Asteroideae, Cichorioideae, and *Artemisia*),
109 *Solanum dulcamara* L., *Rumex sanguineus* L., *Urtica radicans* L., *Galium palustre* L.,
110 *Polygonum aviculare* L. etc. while an aquatic-wetland component surrounding the site includes
111 *Carex elata* L., *Equisetum* spp., *Phragmites communis* L., *Sagittaria sagittifolia* L., *Typha*
112 *angustifolia* L. and *T. latifolia* L. (Karadžić et al., 2015). The modern vegetation around the site
113 contains well-preserved riparian deciduous oak and mixed willow-poplar-ash forests with age-
114 old managed oak-hornbeam stands (Kitnaes et al., 2009).

115 **2.4 Historic setting and the context of the LIA**

116 In the Middle Ages, the Sava River Basin, part of “Syrmia”, witnessed a complex interplay of
117 wars, migrations, epidemics, and famines. During the 14th century, this region including
118 Belgrade was under Hungarian rule. While Hungarians held the northern parts of Sava and
119 Danube, the southern Serbian Empire started falling apart against the rising Ottomans through
120 raids-decisive battles from 1360s (Fine, 1994). To resist Ottoman invasion in the Sava and
121 Danube region, the Hungarians retained their rule through connections with the contemporary
122 Serbian Despotate until the early 15th century (Ali, 2012). This turned out to be one of the

123 periods of noticeable prosperity in terms of economy, culture and agriculture (Stoianovich, 1992;
124 Fine, 1994) when the population of Belgrade City and surrounding areas increased to ~40-50,000
125 inhabitants (City of Belgrade, 2016). Several major conflicts between the Hungarian Empire and
126 the Ottomans occurred between 1450s and early-1500s, ultimately resulting in the Ottoman
127 conquest in 1521 CE. The Ottoman Empire ruled the region for the next 150-160 years and
128 institutionalized resource management for its territories, thereby directing the expansion of the
129 settlement and cultivation across the region (White, 2011). Most parts of 16th and 17th centuries
130 was a comparatively peaceful period with noteworthy commercial progress and significant
131 increase in population (McEvedy and Jones, 1978). Towards the end of the 17th century, the
132 Ottoman Empire started experiencing a major crisis associated with increasing economic turmoil
133 and social unrest within several parts of its territories (White, 2006). During the 17th-18th
134 centuries, this Sava and Danube confluence region was part of the battlefield for constant
135 Ottoman and Habsburg confrontations, resulting in substantial emigration from the region
136 (Mitchell and Kicosev, 1997). This continual inward and outward flow of people as well as
137 internal migrations in the Central Balkans over these centuries caused social changes, e.g.
138 abandonment of marginal lands, transition from wheat to barley and spelt wheat, and from
139 viticulture to plum growing (Mrgić, 2011). During the hardest times, subsistence strategies
140 shifted from agriculture to itinerant animal husbandry-cattle trades (Milojević, 1954).
141 Notwithstanding their attempts, the Ottomans were unable to retain their Balkans territories and
142 consequently, Serbia, like most Balkan countries, became an independent principality around
143 1830-50 CE (Ali, 2012). Following the departure of the Ottomans c. 1850s, a significant
144 population rise was recorded in the region (McEvedy and Jones, 1978; Palairat, 1997).

145

146 **3. Materials and methods**

147 **3.1 Core acquisition**

148 Using the modified Livingstone piston corer (Wright et al., 1984), a 2.57 m sediment core was
149 extracted from the center of the Zivaca oxbow (hereafter, ZO) at a water column depth of 2 m.
150 After recovery, the core was described in the field and was refrigerated at 2-3°C until processing.

151 **3.2 Core sampling, lithological and geochemical analyses**

152 The core was carefully split and photographed prior to sampling. One core half was described for
153 lithology using Munsell soil color chart and was sampled at 8-10 cm intervals for loss-on-
154 ignition (LOI), pollen and micro-charcoal analyses. The LOI procedure was performed according
155 to Dean (1974), where the samples were dried overnight at 100°C to estimate moisture content
156 and then burned at 550°C for 2 hours to obtain the percentages for organic and inorganic content.

157 Geochemical analysis of the archived half of the core was performed using an InnovX
158 Olympus Delta DC-4000 multibeam XRF analyzer at the Environmental Sciences Analytical
159 Center, Brooklyn College of CUNY. Three or more readings were taken at 1-cm intervals with a
160 counting time of 90s and acceleration intensities of 15-40 kV. The values were averaged for each
161 depth (except for lead (Pb)), the five-point moving averages were used for final data analysis.
162 Because the sediment matrix is characterized by variable water content and grain size
163 distributions, the count rates obtained for individual elements can be used as semi-quantitative
164 estimates of their relative concentrations (Aufgebauer et al., 2012). Only select elements
165 including Pb, potassium (K), titanium (Ti), and calcium (Ca) are discussed in this record. Pb is
166 used as a chronological marker in relation to its decline associated with phasing out to unleaded
167 gasoline in the region (Renberg et al., 2001). K and Ti indicate the degree of terrigenous silicate
168 input and soil erosion in the lake settings and act as proxy for physical weathering in the

169 catchment (Arnaud et al., 2012; Francke et al., 2013). Sedimentary Ca reflects changes in
170 hydrological processes, climate, and ecology (Boyle, 2001); decrease in rainfall/fluvial
171 deposition results in lower Ca inputs (Leng et al., 2013).

172 **3.3 Palynological and charcoal analyses**

173 Sediments (~3-4 cm³) sampled for pollen and charcoal analyses were processed using standard
174 sieving (120 and 7 µm), followed by chemical procedures involving KOH, HCl, HF, acetolysis
175 ethanol and tertiary butyl alcohol washes, and immersion in silicone oil (Faegri et al., 2000).
176 Known quantities of *Lycopodium* spores were added to each sample prior to chemical treatment
177 to calculate pollen and charcoal influxes (Stockmarr, 1971). Identification of pollen-spores was
178 done under 400x magnification, using the reference slides from the Laboratory of Palynology of
179 the University of Novi Sad, Lamont Doherty Earth Observatory (LDEO) and from published
180 pollen keys (Moore et al., 1991; Reille, 1999). Pollen recovery varied substantially throughout
181 the core and no pollen was preserved in the bottom segment of the core (220-257 cm). A
182 minimum of 300 terrestrial pollen grains was counted for most depths between 0 and 210 cm.
183 The percentages of arboreal and non-arboreal taxa are based upon the sum of terrestrial pollen
184 and unidentified pollen. Aquatic pollen-spores were counted in addition to the terrestrial pollen
185 and their percentages were calculated from respective sums. Microscopic charcoal was counted
186 for the same slide area as that for the pollen. The size criterion of >50 µm was applied to
187 charcoal counting to avoid confusion with opaque mineral pieces (Clark and Patterson, 1984)
188 that are abundant in this record.

189 **3.4 REVEALS modelling**

190 The pollen–vegetation relationship is not straightforward and depends on the size and type (lake
191 or bog) of the sedimentary basin, differences in the pollen productivity, and dispersal

192 characteristics of taxa (Sugita, 2007; Fredh et al., 2012). To remove these biases, the REVEALS
193 model (Sugita, 2007) was employed to translate pollen percentage data into regional vegetation
194 composition, which, in turn, estimates forested and open land fractions within 50 km surrounding
195 the site. Pollen productivity estimates (PPEs) and the fall speed for 27 terrestrial taxa (17 woody,
196 10 herbaceous; Table 1) were obtained from the literature, including estimates from Bulgaria and
197 the Czech Republic (Bodmer, 1922; Filipova-Marinova et al., 2010; Abraham and Kozáková,
198 2012; Mazier et al., 2012). The REVEALS modelling was implemented using ‘REVEALSinR’
199 function within the R package, DISCOVER (R Core Team, 2014; Theuerkauf et al., 2016). The
200 results were plotted using TILIA Graph (Grimm, 1992).

201 The common pollen types with known PPEs that were excluded from the REVEALS are
202 Ericaceae, Asteroideae, Cichorioideae, *Secale*, and Cyperaceae. The first three were excluded,
203 only after the first model run produced their unrealistically high vegetation estimates (8-10 times
204 that of their respective pollen percentages). This may be due to low PPE values of the two
205 Asteraceae members as well as the entomophilous nature of these taxa; the latter could be
206 responsible for aberrations within the REVEALS’s pollen dispersal function built primarily for
207 wind-pollinated pollen (Mazier et al., 2012). In this context, estimates of other insect-pollinated
208 taxa (e.g. *Acer*) were carefully assessed in the test run. *Acer* produced the REVEALS estimates
209 approximately twice its respective pollen percentage, the pattern shown by some wind-pollinated
210 herbaceous taxa (e.g. Poaceae), thus it could not be attributed to its entomophilous nature.
211 Importantly, unlike other entomophilous taxa which are minor in counts, *Acer* is the second-most
212 dominant tree throughout the record (5-15% of pollen percentages; Fig. S1), exemplifying its
213 inherent presence within the Pannonian forest steppes (See Section 2.3). Since the land cover
214 reconstructed using the REVEALS always adds up to 100% and taxa that are not included in the

215 model reconstruction are completely ignored, the elimination of *Acer* would have resulted in a
 216 seriously underestimated, inaccurate forest cover. Therefore, it was retained in the final model
 217 run. *Secale* is usually treated separately from Cerealia in the REVEALS reconstruction due to its
 218 higher PPE (3.02) as compared to that of (1.85) autogamous cereals including *Triticum*,
 219 *Hordeum*, and *Avena* (Mazier et al., 2012). The ZO record, however, shows either its complete
 220 absence or negligible proportions as compared to other Cerealia members, hence it was not
 221 treated separately but as a part of the Cereals group. Cyperaceae was excluded due to its possible
 222 overrepresentation as a result of the prevalence of wetland conditions around the site.

223

224 **Table 1** Pollen fall speed, pollen productivity estimates (PPEs) relative to Poaceae and standard
 225 error estimates (SE) for 27 taxa used in the REVEALS model. Data obtained from: 1- Mazier et
 226 al., (2012), 2- Abraham and Kozáková, (2012), 3- Bodmer, (1922), and 4 - Filipova-Marinova et
 227 al., (2010)

Pollen taxa	Fall speed (ms ⁻¹)	PPE	SE	Citation
<i>Abies</i>	0.12	6.88	1.44	1
<i>Acer</i>	0.056	0.8	0.23	1
<i>Alnus</i>	0.021	2.56	0.32	1
<i>Betula</i>	0.024	3.09	0.27	1
<i>Carpinus</i>	0.042	3.55	0.43	1
<i>Corylus</i>	0.025	1.99	0.2	1
<i>Fagus</i>	0.057	2.35	0.11	1
<i>Fraxinus</i>	0.022	1.03	0.11	1
<i>Juniperus</i>	0.016	2.07	0.04	1
<i>Juglans</i>	0.037	1.23 [†]	0.3	3, 4
<i>Picea</i>	0.056	2.62	0.12	1
<i>Pinus</i>	0.031	6.38	0.45	1

<i>Quercus</i>	0.035	1.76	0.2	2
<i>Salix</i>	0.022	1.22	0.11	1
<i>Sambucus</i>	0.013	1.3	0.12	2
<i>Tilia</i>	0.032	1.36	0.26	2
<i>Ulmus</i>	0.032	1.27	0.05	1
Amaranthaceae	0.019	4.28	0.27	2
Apiaceae	0.042	0.26	0.01	1
<i>Artemisia</i>	0.025	2.77	0.39	2
Cerealia	0.06	1.85	0.38	1
<i>Galium</i>	0.019	2.61	0.23	1
<i>Plantago lanceolata</i>	0.029	3.7	0.77	2
Poaceae	0.035	1	0	1
Ranunculaceae	0.014	1.96	0.36	1
<i>Rumex acetosa</i>	0.018	2.14	0.28	1
<i>Urtica</i>	0.007	10.52	0.31	2

228 † *Juglans* PPE (originally calculated in relation to *Quercus*) were recalculated in relation to
 229 Poaceae.

230

231 3.5 Rarefaction analysis

232 Rarefaction analysis enables a comparison of taxon richness between samples of different size by
 233 standardizing pollen counts to a single sum (Birks and Line, 1992; Birks et al., 2016). To render
 234 diversity changes within vegetation units through time (Birks and Birks, 2008; Feurdean et al.,
 235 2012), rarefaction analysis was applied to the raw terrestrial pollen dataset using EstimateS 9.1.0
 236 (Colwell, 2013). Raw pollen data was used instead of REVEALS estimates, because the limited
 237 number of herbaceous taxa with known PPEs could have underestimated past diversity changes.
 238 All terrestrial pollen were included and the lowest pollen count was used for the standardization
 239 of the size of the pollen counts for each sample. A few pollen-deficient samples without the

240 threshold pollen sum were excluded from the analysis. The most robust estimate of palynological
241 richness obtained through rarefaction is the expected number of taxa, $E(S_n)$ (Heck et al., 1975;
242 Gotelli and Graves, 1996); these values were plotted against respective depths and correlated
243 with their pollen, charcoal and geochemical counterparts.

244 **3.6 Chronology**

245 The age model for the ZO core is based on nine accelerator mass spectrometry (AMS) ^{14}C dates
246 measured at the Center for Accelerated Mass Spectrometry (CAMS), Lawrence Livermore
247 National Laboratory. A variety of macrofossils were selected for AMS dating after wet sieving
248 of 3-4 g of sediment through 500 and 250 μm screens. Seeds were identified using the Peteet
249 seed collection at LDEO. Due to unavailability of sufficient plant materials towards the bottom
250 of the core, three freshwater gastropod shell samples were used for dating; two of these samples
251 were picked along the same depths with plant-animal remains. The depths, types of macrofossils
252 dated and associated uncalibrated and calibrated ages are presented in Table 2. A few ^{14}C age
253 reversals as well as age inconsistencies were encountered across the depths, which were
254 considered while constructing the reliable age model. Since the core was extracted in the year
255 2012, the core top was set at 2012 CE and the legitimacy of this assumption is discussed in
256 relation to changes in atmospheric Pb deposition in the sediments (See Supplementary Content).
257 An age-depth model (Table 2; Fig. 2) was constructed using a Bayesian approach implemented
258 in Bacon 2.2 (Blaauw and Christen, 2011), based on the IntCal13 calibration curve (Reimer et
259 al., 2013) and prior information assuming a mean accumulation rate of 2 yr/cm and accumulation
260 shape 1.5.

261

262 **Table 2** AMS ^{14}C dates from selected macrofossils, the ZO core. Selected dates used in Bacon
 263 2.2 (Blaauw and Christen, 2011) are shown by an asterisk (*) and the selection criteria are
 264 discussed in detail in the Supplementary Content.

CAMS code	Sample depth (cm)	Materials dated	$\delta^{13}\text{C}$	Uncalibrated ^{14}C year BP	Calibrated 2-sigma age range (cal. CE)	Bacon age (cal. CE)
168940	13	1 twig fragment	-25	335±30	1474-1641	
169242	91	Bark and unidentified seed fragments	-25	370±60*	1604-1811	1674
168941	97	Twig fragment	-25	380±30*	1588-1794	1653
170778	140	1 Asteraceae seed epidermis, leaf fragments	-25	430±70*	1481-1666	1547
170779	170	Apiaceae seed parts, leaf fragments, beetle wing, fish bone remains	-25	400±30*	1427-1597	1480
170780	170	Unidentified shell pieces	0	905±30	1037-1193	
169243	234	Fish vertebra, bone fragment, leaf fragments	-25	330±30	1478-1642	
169244	234	Gastropod shell fragments	-25	580±30*	1274-1414	1331
163355	240	Gastropod shell fragments	-25	800±30*	1259-1395	1316

265

266 4. Results

267 4.1 Lithology and age model

268 The ZO core is composed of alternating sequences of clay, silty clay, and silt varying between
 269 greyish brown and olive grey hues (Fig. 3; Table 3). The complete absence of coarser grained
 270 sediments (e.g. sand) throughout the core is indicative of the lack of major runoff into the lake

271 while it is protected from flooding of the Sava main channel through a levee structure (Kitnaes et
 272 al., 2009). The sediment accumulation is continuous and the boundaries between sediment sizes
 273 are largely gradational. Two distinctive shell layers exist in the lower segment of the core, first
 274 between 244 and 232 cm and the second at around 170 cm.

275

276 **Table 3** Lithostratigraphic description of the ZO core.

Depth (cm)	Lithological units
0-12	Dark olive gray (5Y 3/2) clay
12-25	Light brownish (2.5Y 6/2) silty clay
25-35	Olive gray (5Y 4/2) clay
35-62	Brown (10YR 5/3) silt with an olive gray (5Y 4/2) clay lens at around 50 cm
62-92	Grayish brown (10YR 3/2) silty clay with a dark olive gray (5Y 3/2) clay lens at around 70 cm
92-115	Dark olive gray (5Y 3/2) clay
115-230	Dark grayish brown (10YR 4/2) silty clay interspersed with dark gray (2.5Y 3/2) clay lenses; shells present at 170 cm
230-257	Olive brown (2.5Y 4/3) silt with a shell zone between 232 and 244 cm

277

278 The low amount of organic matter (<7%; Fig. 3) and the limited types of materials that
 279 were available for AMS dating posed challenges in constructing a reliable age-depth for the ZO
 280 core (Table 2, Fig. 2). Six out of nine AMS dates are used for the final age model for the ZO core
 281 (Table 2) along with the atmospheric Pb decline (11 cm = c. 1990 CE; Fig. 2a), and the core top.
 282 The detailed discussion on the selection criteria of the AMS dates as well as the use of Pb as a

283 chronological marker is provided in the Supplementary Content. The resulting age model is
284 constructed using Bacon 2.2 (Fig. 2b). As per this chronology, the base can be extrapolated to c.
285 1262 CE. The multi-proxy analyses of the upper 210 cm spanning about 600 years (~1370-2012
286 CE) are presented here.

287 **4.2 Trends in vegetation cover, taxon richness, micro-charcoal and geochemistry**

288 Regional vegetation cover estimated by the REVEALS model is presented along with respective
289 pollen percentages in Fig. 4. Four major ecological zones are distinguished for the ZO sequence,
290 which correspond with CONISS-based pollen assemblage zones (PAZs in Supplementary Fig.
291 S1). The composite diagram of the ZO sequence has the REVEALS-based forested, open land
292 and cropland estimates, palynological richness, pollen and charcoal influxes, and geochemical
293 indicators juxtaposed with the historic timeline (Fig. 5).

294 **4.2.1 Zone ZO-1 (210-140 cm; ~1373-1525 CE)**

295 Subzone ZO-1a (210-190 cm; 1373-1418 CE) corresponds to a modest decline in the REVEALS
296 estimates of forest cover (68 to 62%; Fig. 5). *Acer* (25%) and *Quercus* (18%) remain the most
297 dominant taxa (the order is opposite in the pollen data; Figs. 4 and S1); both decline (13%)
298 towards the end of the subzone. Unlike their dominant counterparts, many deciduous trees
299 including *Fagus*, *Fraxinus*, *Carpinus*, *Tilia*, and *Ulmus* either increase or maintain steady
300 REVEALS estimates. While other conifers are either absent or <1%, *Juniperus* bears 5% of the
301 land cover at the start of zone but subsequently declines. The shrub cover is of 6-13% with an
302 *Alnus* peak (8%) at 200 cm. Poaceae (25-30%; 15-18% as a pollen percentage) is the main
303 constituent of the open land cover averaging 33% (Fig. 4). Herbaceous taxa such as
304 *Amaranthaceae*, *Apiaceae*, *Ranunculaceae*, *Plantago*, and *Rumex* appear in minor proportions.
305 An anthropogenic component of the landscape includes a cropland of 2-6%, highest *Juglans*

306 estimates (4%), and little to no microscopic charcoal (Figs. 4-5). The palynological richness is
307 steady at 52 at 190-200 cm; pollen-deficient 210 cm-sample without the threshold pollen sum
308 could not produce the $E(S_n)$. The pollen influx displays a plodding decrease. This sub-zone
309 embeds high values of K and Ti while Ca shows a fluctuating concentration.

310 Subzone ZO-1b (190-140 cm; 1418-1525 CE) exhibits a stable forest cover, gradually
311 reaching an extent of 73% in the REVEALS reconstruction (150 cm; Fig. 5). This is largely
312 contributed by increased proportions of most deciduous trees including *Quercus* (13-24%),
313 *Fagus* (3-5%) and *Acer* (22% at 150 cm). The apparent rise in coniferous tree cover is also seen
314 through a sustained presence of *Juniperus* (4-6%) throughout the subzone (Fig. 4). *Salix* expands
315 in this subzone. *Artemisia* peaks (3%) amid declining herbaceous populations. Both cropland as
316 well *Juglans* estimates initially decline (c. 180 cm) but shortly recover and stabilize thereafter.
317 Unlike subzone ZO-1a, microscopic charcoal does not only increase, but reaches its highest
318 value (1600/cm²yr at 160 cm) in the entire sequence. The pollen richness declines from 52 to 48
319 while the pollen influx varies between 12,700 and 27,000/cm²yr. This subzone exhibits
320 continued high concentrations of all the three geochemical indicators, which suddenly decline at
321 170 cm (Fig. 5).

322 **4.2.2 Zone ZO-2 (140-70 cm; ~1525-1734 CE)**

323 Zone ZO-2 is marked by fluctuations in forested and non-forested fractions as suggested by the
324 REVEALS; the overall opening of the landscape is punctuated by surges in the forest cover
325 around 120-100 cm and from 90 cm onwards (Fig. 5). The pollen richness continues to decline in
326 this zone, reaching the count of 40. Pollen influx is highly variable, as are microscopic charcoal
327 accumulation rates. Zone ZO-2 encompasses consistently high values of K, Ti, and Ca with an
328 only exception at 108 cm (Fig. 5).

329 Subzone ZO-2a (140-110 cm; 1525-1591 CE) is characterized by a minor reduction in
330 the forest cover from 67 to 63% up to 120 cm, followed by an abrupt escalation (77%) marking
331 the end of this subzone. The two most dominant trees, *Quercus* and *Acer* show opposite trends;
332 the former decline from 24% to 14% while the latter exhibit its maxima (34%; 15% as a pollen
333 percentage) at 110 cm. *Fagus* shows its maximum estimates (6%) at the start of this subzone;
334 overall all minor deciduous trees either maintain steady or slightly higher estimates. Conifers
335 considerably decline in this subzone. The expansion in the shrub component from 5 to 11% at
336 the end of the zone is tied with an *Alnus* peak; *Sambucus* disappears (Fig. 4). While a few
337 herbaceous taxa (e.g. *Artemisia*, *Apiaceae*, *Galium*, *Ranunculaceae*) seem to vanish/decline in
338 this zone, Poaceae (34%), Amaranthaceae (2%), *Plantago* (2%), and *Rumex* (1%) contribute to
339 the opening of the landscape. As compared to the subzone ZO-1b, the cropland cover is slightly
340 lower but steady, accompanied by a *Juglans* peak and abruptly diminishing micro-charcoal
341 influxes with their minimal values in the entire sequence (950 to 30/cm²yr; Fig. 5).

342 Subzone ZO-2b (110-70 cm; 1591-1734 CE) can be easily distinguishable from the
343 earlier subzone based on the significant expansion of the open landscape (21 to 49%; Fig. 5).
344 This is due to substantial rise in Poaceae (42-46%, 26-28% as a pollen percentage) around 100-
345 90 cm (Fig. 4). With a few exceptions, herbaceous taxa increase as compared to the previous
346 subzone; *Plantago* and *Artemisia* ascend with the latter showing its maximum estimates (4%) in
347 the spectrum. Amaranthaceae show maximum REVEALS estimates (3%) but Poaceae
348 deteriorates at the end of the subzone/Zone 2. The extensive mid-zone reduction in the forest
349 cover (49-50%) is corroborated by the waning of almost all temperate deciduous as well as
350 coniferous trees (Fig. 4). The only exceptions are *Juniperus* and *Salix*, which show a continued
351 growth throughout the subzone. *Juniperus* reaches its maximum estimates of 8%. From 90 cm

352 onwards, the tree cover begins to expand; the notable features in this process include the
353 increased estimates of *Fraxinus* (12%) and *Fagus* (4%) at 80 cm. The peaks of *Ulmus* (8%),
354 *Alnus* (7%), and *Pinus* (4%; 8% as a pollen percentage) marks the end of the Subzone ZO-2b;
355 *Picea* reaches 1% for the first time in the sequence. The cropland further shrinks (<1%) and
356 *Juglans* is almost nonexistent in this subzone. After its complete absence for the earlier part of
357 the subzone, microscopic charcoal reemerges at 90 cm and continues thereafter with $\sim 500/\text{cm}^2\text{yr}$
358 (Fig. 5).

359 **4.2.3 Zone ZO-3 (70-20 cm; ~1734-1950 CE)**

360 In ZO-3, forest cover gradually expands up to an average of 69% (maximum 76%; Fig. 5).
361 *Quercus* exhibits its maximum REVEALS estimates (26%) in the entire sequence; however, its
362 rise does not continue upcore (Fig. 4). A similar declining upcore trend is indicated by *Acer* as
363 well as *Fraxinus*; the former progressively increases up to 31% (12% as a pollen percentage at
364 30 cm) before waning. Both *Ulmus* and *Tilia* show notable rises in this zone while *Fagus* appears
365 sporadically with estimates lower than that of the previous zones. All conifers decrease around
366 50 cm and *Pinus* and *Juniperus* partially recover towards the top of the zone (Fig. 4). All shrubs
367 show fluctuating estimates: *Salix* shows its maximum estimates (6%) around 30 cm but
368 subsequently declines while initially patchy *Corylus* also increases to 6%, marking the end of the
369 zone. Contracted grasslands range only 22-33% in the REVEALS reconstruction (Fig. 4). Their
370 expansion (44%), however, is seen at the end of the zone with increases in Poaceae (averaging to
371 24%; 43% at 20 cm). Amaranthaceae and *Plantago* maintain continuous curves (with a small
372 setback at 50 cm) along with the intermittent presence of all other herbaceous taxa. A moderate
373 increase in the cropland cover as well as in *Juglans* is visible only from 50 cm to the present.
374 Palynological richness curve has a steady decline in this zone, signifying a loss of almost 2-3

375 taxa. Pollen influx is the lowest (1000-3400/cm²yr) in the entire sequence whereas micro-
376 charcoal accumulation values ranges between 410 and 500/cm²yr, slightly less than the Subzone
377 2b. Zone ZO-3 includes the steadily high K, Ti and Ca concentrations with slight variations (Fig.
378 5).

379 **4.2.4 Zone ZO-4 (20-0 cm; ~1950-2012 CE)**

380 In Zone ZO-4, the forest cover expands and stabilizes at 62% from 10 cm to the present at the
381 expense of the shrinking grasslands. The REVEALS estimate of *Carpinus betulus* demonstrates
382 a markedly increase from the base of the zone with its distinctive mid-zone peak (8%; 12% as a
383 pollen percentage) along with *Betula* (7%, 9% as a pollen percentage). Both major deciduous
384 trees, *Quercus* and *Acer* decline in this zone with their minimum REVEALS estimates (10%) in
385 the sequence. *Fraxinus* gradually increases up to 14% (7% as a pollen percentage), becoming the
386 most dominant tree in the region. *Fagus* continue to appear patchy in this zone whereas *Tilia* and
387 *Ulmus* rather fluctuate. *Juniperus* retains similar values from the previous zone while the modest
388 but continuous estimates for the other three conifers coexist for the first time. While Poaceae
389 gradually wane (26%) in ZO-4, Amaranthaceae upsurges along with slight rise in some weedy
390 types of herbaceous pollen including *Plantago* and Apiaceae. The cropland marginally increases
391 from 10 cm onwards, as does *Juglans* cultivation. Palynological richness declines sharply in the
392 region; the plunge is more distinct from 10 cm indicating rapid loss of plant biodiversity over a
393 short period. Pollen influx is almost triple (7500-10,000/cm²yr) as compared to the previous
394 zone. Micro-charcoal influx increases upcore (430 to 860/cm²yr). Zone ZO-4 captures a clear
395 descending trend in K and Ti but an increase in Ca concentrations.

396

397 **5. Discussion**

398 **5.1 Vegetational thresholds for interpreting REVEALS-based landcover changes in the**
399 **Sava Region**

400 The ZO core delineates the environmental history of the Sava Region-Central Balkans that is
401 characteristically defined as a Pannonian forest-steppe zone. In order to have a thorough,
402 accurate interpretation of the paleoenvironmental changes in this region, it is essential to note
403 potential sources of uncertainties in the REVEALS reconstruction and establish more realistic
404 vegetational thresholds. Previous studies (Nielsen et al., 2012; Kuneš et al., 2015; Feurdean et
405 al., 2016) point out certain caveats in the REVEALS reconstruction of forested and non-forested
406 fractions; those discussed specifically in the context of Romanian lowlands appear to hold true
407 for the Sava Region as well: (1) The REVEALS assumes the homogeneity of the vegetation at
408 regional scales with similar vegetation boundaries but without any ecotones (Sugita, 2007). In
409 the Sava Basin, forests are more dominant in the south along the slopes of Dinaric mountain
410 massifs whereas the northern low-lying parts (except Fruska Gora forests) are predominantly
411 grasslands-croplands (Fig. 1; also see Section 2.1). When such variations exist, the vegetation
412 reconstruction in the REVEALS is likely to be more impacted by the local setting than the model
413 predicts and often underestimates the overall extent of the forest cover (Feurdean et al., 2016).
414 This might also be true for croplands in the Sava Basin that are more prevalent in the lowlands,
415 mostly along the river banks. For example, a disparity can be spotted between the expanse of
416 present-day crop fields surrounding the Zivaca Oxbow-Sava River in Fig. 1c and the present-day
417 REVEALS estimates (3%) of the regional cropland in Fig. 5. (2) Certain assumptions in the
418 REVEALS could lead to the overestimation of non-forested cover. First, Poaceae includes
419 several taxa that are usually prevalent in grasslands, but can also be present in other vegetation
420 settings in the Pannonian forest steppe zones (e.g. understory vegetation in woodland, weeds in

421 cropland). Such bifurcation, however, cannot be expected from the REVEALS reconstruction
422 where they are attributed solely to grasslands. Second, the changing degree of grassland
423 management could impact the pollen productivity of Poaceae taxa across time and thus, could
424 implicate a non-linear relationship between pollen and the composition of source vegetation over
425 time (Broström et al., 2008). Managing grasslands in the form of highland pastoralism has been
426 central to the Central Balkan economy since the start of Middle Ages (Popović, 2012), thereby
427 necessitating the cautious limits for discriminating between woodland and grassland scenarios
428 from the REVEALS estimates of the Sava Region.

429 According to Magyari et al., (2010), arboreal pollen (AP) percentages in the wooded
430 steppe zones of Eurasia are frequently <70% (barely exceeds >75%). Thus, for the parts of the
431 Pannonian Plains such as the Sava Region, AP percentages <70% could considered to be a
432 conservative threshold for inferring the predominance of wooded steppe rather than of closed
433 forest in the surrounding landscape (Magyari et al., 2010). In case of pollen-based REVEALS
434 reconstruction, this limit is often relaxed to 55-60% for establishing dominance of woodland
435 over grassland while 30-50% of the forested fractions are interpreted as grassland-dominated
436 landscapes (See for Romanian forest steppe; Feurdean et al., 2016, 2015b). Keeping an eye on
437 probable sources of error and the resultant overestimation of the non-forested cover in the
438 REVEALS discussed above, this study utilizes the uppermost limits of the vegetational
439 thresholds suggested for the Pannonian steppe zones and interprets >75% of REVEALS-based
440 forest cover as fully-developed forest, >60% as a forest steppe setting, and <50% as dominance
441 of grassland/extensively open landscape. Below, the REVEALS-based land-cover changes and
442 relevant changes in the untransformed pollen percentages in the Sava Region are discussed
443 across pre-LIA, LIA and post-LIA time intervals.

444 5.2 Paleoenvironmental history of the Sava Region

445 5.2.1 Pre-LIA wooded steppe and increased cultivation under a steady socio-climatic 446 regime

447 A temperate deciduous forest steppe is evident throughout the pre-LIA (1370-1418 CE; Fig. 4).
448 The regional tree cover existed in the form of assorted oak, maple, and ash strands with scrub
449 populations (e.g. *Alnus*, *Salix*). These taxa usually occupy stretches along the banks of streams
450 and lakes due to their ability to tolerate soils that are temporary waterlogged or flooded
451 (Ellenberg, 2009), thus their continued presence in this interval indicate the availability of
452 sufficient moisture in the lowland as well as along the lake margins. The continued expanse of
453 *Fagus* accompanied by understory shrubs including *Corylus* and *Sambucus* (Fig. 4; also, *Cornus*
454 in Fig. S1) indicate the moderate submontane tree cover along shaded cool valleys, thereby
455 restricting land erosion across the pre-LIA interval (Fig. 5). *Juniperus*, an important component
456 of a borderline forest, decreases in this interval (Fig. 4), which is concurrent with a complete
457 absence of microscopic charcoal (210-190 cm; Fig. 5). Although the increase of *Juniperus* is
458 often associated with human induced fires (Tonkov, 2003; Marinova et al., 2012), its decline
459 cannot necessarily be attributed to the lack of fire management. Hence, it could be argued the
460 decrease in *Juniper* could rather be a climate-driven phenomenon as its presence/increase may
461 often be connected with periods of drying/decreased precipitation in the Balkans-Mediterranean
462 settings (Atherden and Hall, 1999; Caroli and Caldara, 2007; Kouli, 2012; Filipova-Marinova et
463 al., 2013). Thus, the continuous presence of *Fagus*, increase in mesophilous taxa (e.g. *Tilia*,
464 *Ulmus*, and *Carpinus betulus*), and the complete absence of microcharcoal concomitant with the
465 decreasing *Juniperus* extent (Figs. 4-5) could collectively suggest overall stable-warm
466 temperatures and greater moisture availability (e.g. increased precipitation) at least in the growth

467 season (e.g. Magyari et al., 2010). This speculation agrees with the tree-ring based
468 reconstructions of spring/summer precipitation for the eastern Mediterranean (Touchan et al.,
469 2005) with elevated summer rainfall until the 1430s. Such an increase in precipitation in the
470 early 1400s is corroborated by the expansion of the cropland in the region (Fig. 5). This
471 expansion, however, is moderate and could possibly be due to its underestimation in the
472 REVEALS reconstruction (See Section 5.1). Nevertheless, the increase in temperature and
473 moisture-sensitive crop varieties, cereals and *Juglans* (Mercuri et al., 2013; Gogou et al., 2016)
474 indicate the expansion of agriculture-arboriculture in the Sava Region (Figs. 4 and S1), thereby
475 affirming stable-warm temperature and moisture availability in the region.

476 Historically, this pre-LIA interval coincides with a relatively stable Hungarian realm in
477 the region (Fig. 5) and a time of economic and agricultural prosperity with increased migrants
478 (McEvedy and Jones, 1978). The overall increase in the regional population could have resulted
479 in a minor reduction in the deciduous tree cover on lowlands towards the end of the 14th Century.
480 However, more people also mean a sufficient supply of workers for agricultural-pastoral
481 activities, thus this demographic change could have been an asset in terms of providing
482 necessary manpower for sustained agriculture in the presence of the favorable climatic
483 conditions. The minor appearance of secondary anthropogenic indicators including *Plantago*
484 *lanceolata*, Ranunculaceae, and *Rumex* (also, *Polygonum aviculare* and *Humulus/Cannabis* in
485 Fig. S1) indicate that there could have been a supportive line of subsistence related to livestock
486 breeding, ruderalization, and arboriculture (Feurdean et al., 2013; Kuneš et al., 2015).

487 **5.2.2 Human-environmental interactions across the LIA**

488 **5.2.2.1 Stabilized forest cover of the 15th Century and impact of the Ottoman conquest**

489 The earliest century of the LIA in the Sava Region (1418-1525 CE) exhibits a steady forest
490 steppe with the substantial expansion of oaks and maples, dominating the lowlands along with
491 *Fraxinus* and *Salix*. Availability of water required for these communities could be a product of
492 seasonal fluctuations in the water table, which could be attributed to melting of snow in the late
493 spring (Hughes, 2010). Meanwhile, the large swathes of the borderline forest seem to be
494 occupied by *Juniperus* since the early 15th century; increased fire management could have been a
495 primary factor in the substantial growth of this anthropophyte (Figs. 4-5). Also, the overall
496 colder and drier LIA climatic conditions reported for the eastern Mediterranean/Balkans (Popa
497 and Kern, 2009; Buntgen et al., 2013; Cook et al., 2016; Kern et al., 2016) could have also
498 helped the spread of *Juniperus*. The reduction in drought-sensitive trees (e.g. *Tilia*) and crops
499 (e.g. cereals, *Juglans*) is concomitant with the development of *Juniper* strands (180 cm; Fig. 4),
500 however, no such reduction is noticed for *Fagus* in the 15th or early 16th Century CE. Beech
501 forest can sustain colder summers, but is susceptible to continued droughts and/or variability in
502 the summer precipitation (Peterken and Mountford, 1996). Thus, its modest yet unwavering
503 expanse until the early 16th Century CE could infer that if this was a period of increased
504 dryness/decreased summer precipitation on the regional scale, the amplitude of these variations
505 could be moderate for this part of the Balkans. Existing hydro-climate proxy records from the
506 Balkan-Mediterranean region (Hughes, 2010; Zerefos et al., 2011; Zanchetta et al., 2012;
507 Feurdean et al., 2015a; Gogou et al., 2016) attest the intra-/inter-annual variability in the seasonal
508 rainfall since the start of the LIA. Thus, the stable-expanding lowland deciduous tree cover with
509 limited montane vegetation in the Sava Region during 1418-1525 CE could rather account for an
510 episodic nature of the “LIA-like” events (e.g. sporadic drying episodes/reduction in the winter
511 precipitation; Matthews and Briffa, 2005) than overall dry conditions. Since steady/expanding

512 tree canopies often hamper the development of understory vegetation, resulting in a floristically
513 less diverse landscape (Meltsov et al., 2011; Feurdean et al., 2013), the continued reduction in
514 taxon diversity since the start of the LIA seem to capture these ecological changes in the Sava
515 Region (Fig. 5).

516 The likely occurrence of the intermittent dry LIA episodes is corroborated by the
517 lithological changes between 1460s and 1530s, where silty clay is interspersed with clay lenses
518 (170-140 cm; Fig. 3). The lower clastic inputs shown by these intercalations specify decreased
519 land erosion whereas the drop in Ca could partially impart decreased hydrological activity in the
520 catchment from 1460s onwards (Fig. 5). Since the carbonate deposition/shell layer often saturate
521 Ca levels in sedimentary sequences (e.g. Aufgebauer et al., 2012), the decrease in Ca could be a
522 combined product of carbonate crystallization and changing precipitation regimes in this earliest
523 part of the LIA.

524 However moderate, the effects of “LIA-like” episodes coincided with periods of major
525 political conflicts during late 15th and early 16th centuries, intensifying human impact through
526 fires in the Sava Region (Fig. 5). While micro-charcoal signify regional fires, its abundance
527 could be amplified by local fires (Whitlock and Larsen, 2001). Extensive burning of villages and
528 landscape is reported for the Sava Region during the Ottoman-Hungarian confrontations and the
529 Ottoman conquest in 1521 (Mrgić, 2011). Two major fire signals c. 1480s and 1520s CE (Fig. 5)
530 seem to corroborate such local burnings on top of regional fire management (e.g. maintenance of
531 pastureland, burn of crop residues). The cropland barely increased in this century but certain
532 highland pastoral indicators continued to exist (e.g. *Artemisia*, *Plantago*, and *Rumex*; Fig. 4),
533 thus a major motivation behind fire management could have been to increase grazing areas rather
534 than agricultural areas. The expansion of grazing in connection with the Turkish

535 invasion/Turcoman nomads has also been identified for other parts of the Balkans (Izdebski et
536 al., 2015; Gogou et al., 2016). Apparently, changing socio-political scenarios across the Balkans
537 could have motivated peasants to intensify fires and grazing in the highlands under the earliest
538 spell of the LIA.

539 **5.2.2.2 Early LIA dwindling woodland-stressed agriculture under the stable Ottoman** 540 **regime**

541 The early-mid 16th Century witnessed a slight opening of landscape in the Sava catchment (ZO-
542 2a; Fig. 5). This was apparent in case of the temperate deciduous lowland vegetation, which
543 transformed into denser maple canopies. *Acer* is not only a primary constituent of
544 thermophile/temperate deciduous forest-steppes, but also occur as a part of azonal/relict
545 vegetation scattered in the beech and beech-fir belts over 1000 a.m.s.l. (Rakonjac and Nevenic,
546 2012). Thus, it is possible that both scenarios could have materialized for *Acer* that persistently
547 grew the later part of the 16th Century, perhaps at the expense of other major trees (e.g. *Quercus*,
548 *Fagus*). During the early-mid 17th Century CE, extensive grasslands dominated the landscape
549 accompanied by herbaceous steppe communities (e.g. *Artemisia* expansion c. 1614-1645 CE,
550 Fig. 4). While most deciduous as well as coniferous tree-shrub cover shrank around this time,
551 *Juniperus* regained its strength to dominate the forest border zones until the early 18th Century
552 CE. Vegetation cover is often reduced before soil erosion ensues, leading to higher clastic inputs
553 into the lakes (Widlök et al., 2012). Extensive land erosion since 1600s corroborate overall
554 fluctuations in the deciduous tree-shrub cover and the expansion of grasslands during the early
555 LIA (Fig. 5). Continued diminution in the taxon diversity is also a product of changing
556 woodland-grassland dynamics throughout this interval.

557 During the 16th and 17th Centuries, the Sava Region was under the stable early Ottoman
558 realm with subsequent population influx (McEvedy and Jones, 1978). This demographic rise
559 could be envisaged as a prime cause for landscape opening in the need of more food production.
560 However, based on normalized annual population estimates for Yugoslavia, Kaplan et al. (2009)
561 argue that the Balkan region continued to maintain low population density as well as
562 deforestation rates until 1750 CE, where highly productive arable lands on non-forested fractions
563 were capable of feeding increased population during the early Ottoman period. Despite being the
564 centerpiece of the Ottoman Empire, the Sava Region shows a modest opening of the landscape
565 and subsequent increase in woodland during the 16th Century CE, at the peak of the Ottoman
566 expansion (ZO-2a; Fig. 5) and agrees with the low regional deforestation signal. The low
567 charcoal influxes as well as gradual reduction in cropland throughout this early LIA interval
568 reveal overall minor human interference, but potential impacts of the LIA climate on the
569 woodland as well as cropland in the region.

570 The 16th and 17th centuries CE in the greater Mediterranean region are characterized by
571 multiannual to decadal variations and several prolonged wet and dry events (Touchan et al.,
572 2005; Nicault et al., 2008). Several well-marked droughts and coldest springs are marked
573 throughout these centuries especially 1540-1575, 1620-1640, and 1645-1665 CE. (Nicault et al.,
574 2008) and during the Last Maunder Minimum i.e. 1675-1715 CE (Xoplaki et al., 2001). Several
575 multiproxy Balkan records present fluctuating precipitation with an overall drying trend in the
576 region; these include records in Serbia (Kulkarni et al., 2016), Romania (Feurdean, 2005;
577 Schnitchen et al., 2006; Feurdean et al., 2015a), Albania (Van Welden et al., 2008; Zanchetta et
578 al., 2012), Macedonia (Francke et al., 2013; Thienemann et al., 2017), Greece/Anatolia (Gogou
579 et al., 2016; Kouli, 2012; Koutsodendris et al., 2017; Luterbacher et al., 2011 and references

580 therein). Thus, the substantial reduction in the forest cover as well as cropland amid a war-less
581 early Ottoman realm of the Sava Region could be tentatively attributed to the drying trend/LIA
582 climatic variability at least until the mid-17th Century CE (Fig. 5). This ecological change,
583 especially the collapse of agriculture/arboriculture, fits within the a characteristic picture of most
584 Ottoman provinces during 1600-1700 CE, where prolonged failures of wheat harvests and
585 subsequent embargoed exports are reported through Ottoman tax records (Purgstall, 1983).

586 The socio-political stressors such as wars, internal and external migrations, epidemics,
587 and famines (Xoplaki et al., 2001; White, 2006) during the late-17th Century CE, however,
588 complicated the situation. According to Mrgić (2011), there was a large-scale depopulation of
589 Northern and Central Serbia from the late-17th Century onwards, mainly because it was a war
590 zone with frequent Habsburg–Ottoman confrontations (1683–99 CE, 1714–18 CE; Fig. 5). Low
591 population density and the abandonment of agriculture during this time resulted in the
592 reforestation in the region, which earned it the name, “Sumadija” (literally, “Woodland”;
593 Milojević, 1954). The restoration of the forest cover around 1690 CE (Fig. 4) could be part of
594 this ecological change in the Sava Region, when the riparian tree-shrub component (e.g.
595 *Fraxinus*, *Alnus*, *Salix*) expanded along inundated lake margins. The further decline in
596 agriculture towards the end of 17th Century could be a collective artifact of the insufficient
597 moisture of the LIA weather patterns as well as instable socio-political regimes of the time.
598 Moderate charcoal influx values during 1645-1734 CE (Fig. 5) and the continuous presence of
599 *Plantago* (Fig. 4; rise in *Pedicularis* and Ericaceae in Fig. S1) together indicate that the use of
600 fire in landscape management returned in the region as people may have temporally reverted to
601 their age-old highland pastoral subsistence in these climatically-socially difficult times (Mrgić,
602 2011).

603 **5.2.2.3 Stable woodland/wooded steppe during the latter phase of the LIA**

604 The late-LIA interval (1730-1850 CE) shows a gradual expansion of forest steppe region that
605 continue till the early-1900s (Fig. 5). Both major constituents of the lowland deciduous forest,
606 oaks and maples continued to dominate the landscape while other components of the riparian
607 vegetation (e.g. *Alnus*, *Fraxinus*) show a subordinate presence, suggesting the moist banks of the
608 oxbow lake under the study. The sustained rise in the drought-sensitive mesophilous tree taxa
609 (e.g. *Tilia*, *Ulmus*) is also visible in the Sava Region, which is often associated with rising
610 temperatures during the growing season and increasing moisture availability at the regional level
611 (e.g. Panagiotopoulos et al., 2013). Similar ecological change during this timeframe (1720-1850
612 CE) is reported for southern catchments of the Sava in Serbia (Kulkarni et al., 2016) and is
613 linked to the more moderate, less transient phase of the dry-cold LIA in the Balkans (e.g.
614 dendrochronological records in Bosnia (Poljanšek et al., 2013) and Romania (Popa and Kern,
615 2009; Popa and Bouriaud, 2014). Although *Ulmus* is also part of seasonally inundated alder-ash
616 forests in the Sava Region (See Section 2.3), the rise in *Tilia* on both sides of the Sava river
617 could be tentatively attributed to more stable weather patterns. The modest recovery of the
618 cropland cover and *Juglans* cultivation (Fig. 4) could also indicate the moderate shifts in
619 moisture availability towards the end of the LIA (early 19th Century CE). The latter phase of the
620 LIA, however, coincides with the late Ottoman period with continued Habsburg-Ottoman
621 confrontations (e.g. 1736–39 CE, 1788–92 CE), resultant outmigration and further reforestation
622 of the Sava Region (Mrgić, 2011). Hence, in addition to the less-transient phase of the LIA, the
623 higher forested cover as well as discontinuous cultivation in the region could potentially be due
624 to lack of human intervention/care.

625 Itinerant animal husbandry-cattle trades is found to be an important source of subsistence
626 in parts of Balkans during these dynamic socio-political times (Milojević, 1954; Mrgić, 2011).
627 The uniform land clearance, continuous presence of grazing-ruderal indicators (e.g. *Plantago*,
628 *Apiaceae*, *Rumex*), and decrease or patchy appearance of most major montane/sub-montane taxa
629 (e.g. *Fagus*, *Abies*, *Betula*, *Carpinus* except *Pinus*) agree with this speculation (Figs. 4-5). While
630 the early LIA climate and human response to the climate significantly impacted the montane
631 forest cover in the Sava Region, the human exploitation of highlands continued in the late LIA
632 primarily for pig rearing (Palairret, 1997). In this context, the increased and stable *Pinus* expanse
633 throughout the 18th Century (Fig. 4) is an interesting phenomenon, which could be explained
634 using two scenarios: First, unlike its montane counterpart (e.g. beech-fir), *Pinus* is an early-
635 succession, hardy tree, capable of thriving in drier-cooler conditions (Panagiotopoulos et al.,
636 2013). Secondly, it is plausible that people could have preferred clearance of beech-fir over pines
637 to exploit timber and feed a large animal population (Palairret, 1997). Thus, the maintenance of
638 pine forest cover during the late LIA could have resulted from both natural and unintentional
639 human influences. The overall reduction in highland vegetation and abandoned fields located on
640 hills and river terraces would have quickly lost much of their soils; steadily high K and Ti
641 concentrations during 1730s-1850s confirm higher rates of land erosion (Fig. 5). The alternating
642 sequences of clay, silty clay and silt (70-40 cm; Fig. 3) indicate changes in lake levels, thereby
643 explaining short-term fluctuations in Ca concentrations (Fig. 5).

644 **5.2.3 Post-LIA/Industrial Era forest steppe zones of the Sava Region**

645 **5.2.3.1 Increased forested cover amid the process of industrialization**

646 The century of 1850-1950 CE marked the end of the LIA/a transition towards the Industrial Era
647 and witnessed further expansion of the forest cover and development of a dense woodland in the

648 Sava Region until the start of the 20th Century (Fig. 5). This ecological change is seen through
649 increased proportions of maple communities outcompeting oaks in the region, which are
650 accompanied by several lowland tree populations. *Juniperus* expands once again to dominate the
651 borderline forest. The retention of overall forest cover since the latter part of the LIA moderately
652 impacted the taxon diversity in the region; the steeper palynological richness curve indicates a
653 slower rate of diminishing taxa (Fig. 5). While the regional climate reconstructions at the close
654 of the LIA indicate higher summer temperatures as well as increased moisture availability for the
655 Balkan-Mediterranean and Europe overall (Luterbacher et al., 2004; Touchan et al., 2005; Griggs
656 et al., 2007; Seim et al., 2012; Poljanšek et al., 2013; Popa and Bouriaud, 2014), none of this
657 seems to have favored woodland expansion in the Sava Region from 1900 CE onwards.
658 Increased population pressures following the exit of the Ottomans c.1850 CE and the subsequent
659 onset of the Industrial Revolution, agricultural developments, and increased trade led to intense
660 deforestation across Eastern Europe (McEvedy and Jones, 1978; Kaplan et al., 2009). Decrease
661 in forest cover in the Sava Region during 1900-1950 CE can be linked to extensive land use by
662 local populations with sustained use of fire practices (Fig. 5). All these are governing factors for
663 intense land erosion in this century as shown by all the geochemical indicators (Fig. 3). The fire
664 signals could also have been amplified especially since the start of the 20th century CE by a
665 series of major wars including the Balkan Wars (1912-13 CE), World War I (1914-1919 CE),
666 and World War II (1939-1945 CE). Amid these adversities, the arboriculture in the region seems
667 to increase moderately while the cereal cultivation occurs over a comparatively lower cropland
668 cover as compared to its LIA and pre-LIA counterparts. Producing more food on the same or
669 lower cropland area could be a combined product of overall stable-warmer temperatures in the

670 20th century and the availability of the better agricultural technologies in the wake of the
671 Industrial Era.

672 **5.2.3.2 Development of present-day forest under the Socialist and post-Socialist scenarios**

673 Much of the post-WWII interval denotes the Socialist period (1950-1990 CE) in the Balkan
674 region. As an imprint of this period of intense production, the forest steppe seems to have
675 competed with grasslands, eventually stabilizing to represent modern-day vegetation around the
676 ZO lake. As a result, taxon diversity continues to wane; the plunge is more distinct from 1990
677 CE indicating a rapid loss of plant biodiversity over a short period (Fig. 5). Today, the site is
678 dominated by riparian oak-hornbeam populations and mixed forests with willow, poplar, and ash
679 along the flooded locales along with small natural wetlands (Kitnaes et al., 2009), while the area
680 surrounding the site is under arable lands (Fig. 1c). All these features are present in the regional
681 landcover reconstruction of the Sava Region with a slight underestimation of the cropland,
682 potentially due to its occurrence within the basin. The marked rises in *Carpinus betulus* and
683 *Betula* (Fig. 4) over the past few decades could be part of the natural forest regime surrounding
684 the site but also a result of establishment of forest reserves and national parks in the vicinity of
685 the study site (e.g. Obedska Bara, Bojcinska suma) and along the Fruska Gora Mountains in the
686 north (Radović and Kozomara, 2011). The process of developing ecological networks has been
687 continuous in Serbia since 1960s, leading to c. 300,000 ha of the protected areas of the day
688 (Sekulić et al., 2012). As an early successional tree, *Betula* could have taken advantage of this
689 available land. A significant decline in land erosion is apparent through low K and Ti inputs
690 since 1950s (Fig. 5). The increased concentration of Ca, however, could be associated with the
691 use of artificial fertilizers on the surrounding croplands.

692

693 **6. Conclusions**

694 Major insights from this new high-resolution Central Balkan record from the Sava Region are:

695 1) The pre-LIA interval (1370-1418 CE) reveals a wooded steppe region and increased
696 cultivation under warmer/stable climatic and socio-political conditions.

697 2) The start of the LIA in the Sava Region could tentatively go back to the early-mid 15th
698 Century, where the expanding lowland forest steppe and limited montane vegetation perhaps
699 indicate “LIA-like” conditions i.e. intra-/interannual variability of the seasonal rainfall.
700 However, the amplitude of these climatic changes seems to be moderate for this part of the
701 Balkans and does not fully account for the regional drying trend. The concurrency of these
702 episodic dry events with the Ottoman conquest of the region could have promoted highland
703 pastoralism as a supporting line of subsistence.

704 3) The early LIA interval (1525-1734 CE) is characterized by dwindling woodland accompanied
705 by extensive land erosion and faltering agriculture. This ecological deterioration amid a war-
706 less early-Ottoman realm could be potentially associated with the drying trend/extreme
707 climatic variability across the early LIA. The noticeable increase in woodland and modest
708 recovery of the cropland cover during the latter phase of the LIA, however, seems to be a
709 collective artifact of the less-transient phase of the LIA and decreased societal stress due to
710 outmigration during the late Ottoman period.

711 4) The post-LIA/Industrial Era interval (1850-2012 CE) in the Sava Region shows an overall
712 increase in woodland and increased agriculture on the LIA-cropland cover until 1900 CE.
713 Following the exit of the Ottomans, increased population pressures and the subsequent onset
714 of the Industrial Revolution, agricultural developments, and increased trade led to intense
715 deforestation in the region during the first half of the 20th Century, which continued during the

716 Socialist period. Modern day forest steppe in the Sava Region seem to have established during
717 the mid-20th Century.

718

719 **Acknowledgments**

720 We are really grateful to Mr. Marko Djuric from nutropetcom for allowing and helping to
721 retrieve the core from Zivaca oxbow lake. We would like to thank Dr. Branko Sikoparia and Dr.
722 Predrag Radisic from the Laboratory of Palynology, University of Novi Sad, Serbia for
723 providing necessary reference pollen slides. Special thanks go to the colleagues from Department
724 of Earth and Environmental Sciences, Brooklyn College of CUNY - Dr. Brett Branco and Dr.
725 Zhongqi Cheng for allowing use of their labs for pollen extraction of the part of the ZO core and
726 Jessica Khaimova for XRFing the core. Discussions with Dr. Jacques-Louis de Beaulieu
727 provided valuable insights into the vegetational history aspect of this manuscript. We also
728 express our gratitude towards two anonymous reviewers, the editor, Dr. Min-Te Chen, and the
729 associate editor, Dr. Alessandra Negri for their constructive recommendations on the earlier
730 versions of the manuscript. This research was supported by PSC CUNY Grant No. 66575-00-44
731 and is part of Charuta Kulkarni's Doctoral Dissertation submitted to the CUNY Graduate Center.
732 This is LDEO contribution no. xxxx.

733 **References**

- 734 Abraham, V., Kozáková, R., 2012. Relative pollen productivity estimates in the modern
735 agricultural landscape of Central Bohemia (Czech Republic). *Review of Palaeobotany and*
736 *Palynology* 179, 1–12. doi:10.1016/j.revpalbo.2012.04.004
- 737 Ali, A., 2012. Ottoman Balkan Conquests: 1250 to 1920: Middle East. In: Stanton, A.L.,
738 Ramsay, E., Seybolt, P.J., Elliott, C.M. (Eds.), *Cultural Sociology of the Middle East, Asia,*

- 739 & Africa: An Encyclopedia. SAGE Publications, Inc., Thousand Oaks, pp. I173–I174.
740 doi:<http://dx.doi.org/10.4135/9781452218458.n92>
- 741 Andric, M., 2016. Human impact on the vegetation of the western Ljubljansko barje in late
742 prehistory (ca. 1000–50 cal. BC). Case study: Vrhnika (Dolge njive). *Arheološki vestnik* 67,
743 259–275.
- 744 Andric, M., Willis, K.J., 2003. The phytogeographical regions of Slovenia: A consequence of
745 natural environmental variation or prehistoric human activity? *Journal of Ecology* 91, 807–
746 821. doi:[10.1046/j.1365-2745.2003.00808.x](https://doi.org/10.1046/j.1365-2745.2003.00808.x)
- 747 Arnaud, F., Révillon, S., Debret, M., Revel, M., Chapron, E., Jacob, J., Giguet-Covex, C.,
748 Poulencard, J., Magny, M., 2012. Lake Bourget regional erosion patterns reconstruction
749 reveals Holocene NW European Alps soil evolution and paleohydrology. *Quaternary*
750 *Science Reviews* 51, 81–92. doi:[10.1016/j.quascirev.2012.07.025](https://doi.org/10.1016/j.quascirev.2012.07.025)
- 751 Atherden, M.A., Hall, J.A., 1999. Human impact on vegetation in the White Mountains of Crete
752 since AD 500. *The Holocene* 9, 183–193. doi:[10.1191/095968399673523574](https://doi.org/10.1191/095968399673523574)
- 753 Aufgebauer, A., Panagiotopoulos, K., Wagner, B., Schaebitz, F., Viehberg, F.A., Vogel, H.,
754 Zanchetta, G., Sulpizio, R., Leng, M.J., Damaschke, M., 2012. Climate and environmental
755 change in the Balkans over the last 17 ka recorded in sediments from Lake Prespa
756 (Albania/F.Y.R. of Macedonia/Greece). *Quaternary International* 274, 122–135.
757 doi:<http://dx.doi.org/10.1016/j.quaint.2012.02.015>
- 758 Birks, H.J.B., Birks, H.H., 2008. Biological responses to rapid climate change at the Younger
759 Dryas–Holocene transition at Krakanes, western Norway. *The Holocene* 18, 19–30.
- 760 Birks, H.J.B., Line, J.M., 1992. The use of rarefaction analysis for estimating palynological
761 richness from Quaternary pollen-analytical data. *Holocene* 2, 1–10.

- 762 doi:10.1177/095968369200200101
- 763 Birks, H.J.B., Felde, V.A., Bjune, A.E., Grytnes, J.-A., Seppä, H., Giesecke, T., 2016. Does
764 pollen-assemblage richness reflect floristic richness? A review of recent developments and
765 future challenges. *Review of Palaeobotany and Palynology* 228, 1–25.
766 doi:10.1016/j.revpalbo.2015.12.011
- 767 Blaauw, M., Christen, J.A., 2011. Flexible paleoclimate age-depth models using an
768 autoregressive gamma process. *Bayesian Analysis* 6, 457–474. doi:10.1214/11-BA618
- 769 Blaauw, M., Christen, J.A., 2013. Bacon manual – v2.2.
- 770 Bodmer, H., 1922. Über den Windpollen. *Natur und Technik* 3, 294–298.
- 771 Boyle, J.F., 2001. Inorganic Geochemical Methods in Palaeolimnology. In: Last, W.M., Smol,
772 J.P. (Eds.), *Tracking Environmental Change Using Lake Sediments*. Springer Netherlands,
773 Dordrecht, pp. 83–141. doi:10.1007/0-306-47670-3_5
- 774 Bradley, R.S., Jones, P.D., 1992. When was the “Little Ice Age”? In: *Proceedings of the*
775 *International Symposium on the Little Ice Age*. pp. 1–4.
- 776 Bradley, R.S., Jones, P.D., 1993a. “Little Ice Age” summer temperature variations: their nature
777 and relevance to recent global warming trends. *The Holocene* 3, 367–376.
778 doi:10.1177/095968369300300409
- 779 Bradley, R.S., Jones, P.D., 1993b. “Little Ice Age” summer temperature variations: their nature
780 and relevance to recent global warming trends. *The Holocene* 3, 367–376.
781 doi:10.1177/095968369300300409
- 782 Broström, A., Nielsen, A.B., Gaillard, M.J., Hjelle, K., Mazier, F., Binney, H., Bunting, J., Fyfe,
783 R., Meltsov, V., Poska, A., Räsänen, S., Soepboer, W., Stedingk, H. Von, Suutari, H.,
784 Sugita, S., 2008. Pollen productivity estimates of key European plant taxa for quantitative

- 785 reconstruction of past vegetation: A review. *Vegetation History and Archaeobotany* 17,
786 461–478. doi:10.1007/s00334-008-0148-8
- 787 Buntgen, U., Tegel, W., Nicolussi, K., McCormick, M., Frank, D., Trouet, V., Kaplan, J.O.,
788 Herzig, F., Heussner, K.-U., Wanner, H., Luterbacher, J., Esper, J., 2011. 2500 Years of
789 European Climate Variability and Human Susceptibility. *Science* 331, 578–582.
790 doi:10.1126/science.1197175
- 791 Buntgen, U., Kyncl, T., Ginzler, C., Jacks, D.S., Esper, J., Tegel, W., Heussner, K.-U., Kyncl, J.,
792 2013. Filling the Eastern European gap in millennium-long temperature reconstructions.
793 *Proceedings of the National Academy of Sciences* 110, 1773–1778.
794 doi:10.1073/pnas.1211485110
- 795 Caroli, I., Caldara, M., 2007. Vegetation history of Lago Battaglia (eastern Gargano coast,
796 Apulia, Italy) during the middle-late Holocene. *Vegetation History and Archaeobotany* 16,
797 317–327. doi:10.1007/s00334-006-0045-y
- 798 Chapman, J.C., Magyari, E.K., Gaydarska, B., 2009. Contrasting Subsistence Strategies in the
799 Early Iron Age? – New Results from the Alfold Plain, Hungary, and the Thracian Plain ,
800 Bulgaria. *Oxford Journal of Archaeology* 28, 155–187.
- 801 City of Belgrade, 2016. History: Medieval Serbian Belgrade [WWW Document]. URL
802 <http://www.beograd.rs/en/discover-belgrade/201247-medieval-serbian-belgrade/> (accessed
803 2.10.16).
- 804 Clark, J.S., Patterson, W.A., 1984. Pollen, PB-210, and Opaque Spherules: An Integrated
805 Approach to Dating and Sedimentation in the Intertidal Environment. *SEPM Journal of*
806 *Sedimentary Research* 54, 1251–1265. doi:10.1306/212F85B2-2B24-11D7-
807 8648000102C1865D

- 808 Colwell, R., 2013. EstimateS: Statistical estimation of species richness and shared species from
809 samples. Version 9. User's Guide and application. [WWW Document].
810 <http://purl.oclc.org/estimates>. URL <http://purl.oclc.org/estimates>
- 811 Cook, B.I., Anchukaitis, K.J., Touchan, R., Meko, D.M., Cook, E.R., 2016. Spatiotemporal
812 drought variability in the Mediterranean over the last 900 years. *Journal of Geophysical*
813 *Research: Atmospheres* 121, 2060–2074. doi:10.1002/2015JD023929
- 814 Cook, E.R., Seager, R., Kushnir, Y., Briffa, K.R., Büntgen, U., Frank, D., Krusic, P.J., Tegel,
815 W., Schrier, G. Van Der, Andreu-Hayles, L., Baillie, M., Baittinger, C., Bleicher, N.,
816 Bonde, N., Brown, D., Carrer, M., Cooper, R., Čufar, K., Dittmar, C., Esper, J., 2015. Old
817 World megadroughts and pluvials during the Common Era. *Science Advances* 1, 1–9.
818 doi:10.1126/sciadv.1500561
- 819 Cvetkovic, V., Poli, G., Christofides, G., Koroneos, A., Pecksay, K., Eric, V., 2007. Miocene
820 granitoid rocks of Mt. Bukulja (central Serbia): Evidence for pannonian extension-related
821 granitoid magmatism in the northern Dinarides. *European Journal of Mineralogy* 19, 513–
822 532.
- 823 Dean, W.E.J., 1974. Determination of carbonate and organic matter in calcareous sediments and
824 sedimentary rocks by loss on ignition: Comparison with other methods. *Journal of*
825 *Sedimentary Petrology* 44, 242–248. doi:10.1306/74D729D2-2B21-11D7-
826 8648000102C1865D
- 827 Ellenberg, H., 2009. *Vegetation Ecology of Central Europe*. Cambridge University Press,
828 Cambridge, UK.
- 829 Faegri, K., Iversen, J., Kaland, P.E., Krzywinski, K., 2000. *Textbook of Pollen Analysis*, 4th ed.
830 Blackburn Press.

- 831 Feurdean, A., Munteanu, C., Kuemmerle, T., Nielsen, A.B., Hutchinson, S.M., Ruprecht, E.,
832 Parr, C.L., Persoiu, A., Hickler, T., 2016. Long-term land-cover/use change in a traditional
833 farming landscape in Romania inferred from pollen data, historical maps, and satellite
834 images. *Regional Environmental Change* (Online). doi:10.1007/s10113-016-1063-7
- 835 Feurdean, A.N., 2005. Holocene forest dynamics in northwestern Romania. *The Holocene* 15,
836 435–446. doi:10.1191/0959683605hl803rp
- 837 Feurdean, A.N., Tamaş, T., Tanţău, I., Al., E., 2012. Elevational variation in regional vegetation
838 responses to late-glacial climate changes in the Carpathians. *Journal of Biogeography* 39,
839 258–271. doi:10.1111/j.1365-2699.2011.02605.x
- 840 Feurdean, A.N., Parr, C.L., Tantau, I., Farcas, S., Marinova, E., Persoiu, I., 2013. Biodiversity
841 variability across elevations in the Carpathians: Parallel change with landscape openness
842 and land use. *The Holocene* 23, 869–881. doi:10.1177/0959683612474482
- 843 Feurdean, A.N., Galka, M., Kuske, E., Tantau, I., Lamentowicz, M., Florescu, G., Liakka, J.,
844 Hutchinson, S.M., Mulch, A., Hickler, T., 2015a. Last Millennium hydro-climate variability
845 in Central-Eastern Europe (Northern Carpathians, Romania). *The Holocene* 25, 1179–1192.
846 doi:10.1177/0959683615580197
- 847 Feurdean, A.N., Marinova, E., Nielsen, A.B., Liakka, J., Veres, D., Hutchinson, S.M., Braun, M.,
848 Timar-Gabor, A., Astalos, C., Mosbrugger, V., Hickler, T., 2015b. Origin of the forest
849 steppe and exceptional grassland diversity in Transylvania (central-eastern Europe). *Journal*
850 *of Biogeography* 42, 951–963. doi:10.1111/jbi.12468
- 851 Filipova-Marinova, M., Pavlov, D., Coolen, M., Giosan, L., 2013. First high-resolution
852 marinopalynological stratigraphy of Late Quaternary sediments from the central part of the
853 Bulgarian Black Sea area. *Quaternary International* 293, 170–183.

- 854 doi:10.1016/j.quaint.2012.05.002
- 855 Filipova-Marinova, M. V., Kvavadze, E. V., Connor, S.E., Sjögren, P., 2010. Estimating absolute
856 pollen productivity for some European Tertiary-relict taxa. *Vegetation History and*
857 *Archaeobotany* 19, 351–364. doi:10.1007/s00334-010-0257-z
- 858 Fine, J.V.A., 1994. *The Late Medieval Balkans: A Critical Survey from the Late Twelfth*
859 *Century to the Ottoman Conquest*. University of Michigan Press.
- 860 Finsinger, W., Morales-Molino, C., Gałka, M., Valsecchi, V., Bojovic, S., Tinner, W., 2017.
861 Holocene vegetation and fire dynamics at Crveni Potok, a small mire in the Dinaric Alps
862 (Tara National Park, Serbia). *Quaternary Science Reviews* 167, 63–77.
863 doi:10.1016/j.quascirev.2017.04.032
- 864 Francke, A., Wagner, B., Leng, M.J., Rethemeyer, J., 2013. A Late Glacial to Holocene record of
865 environmental change from Lake Dojran (Macedonia, Greece). *Climate of the Past* 9, 481–
866 498. doi:10.5194/cp-9-481-2013
- 867 Fredh, D., Broström, A., Zillén, L., Mazier, F., Rundgren, M., Lagerås, P., 2012. Floristic
868 diversity in the transition from traditional to modern land-use in southern Sweden a.d. 1800-
869 2008. *Vegetation History and Archaeobotany* 21, 439–452. doi:10.1007/s00334-012-0357-z
- 870 Gardner, A.R., Willis, K.J., 1999. Prehistoric farming and the postglacial expansion of beech and
871 hombeam: a comment on Kuster. *The Holocene* 9, 119–121.
- 872 Gogou, A., Triantaphyllou, M., Xoplaki, E., Izdebski, A., Parinos, C., Dimiza, M., Bouloubassi,
873 I., Luterbacher, J., Kouli, K., Martrat, B., Toreti, A., Fleitmann, D., Rousakis, G., Kaberi,
874 H., Athanasiou, M., Lykousis, V., 2016. Climate variability and socio-environmental
875 changes in the northern Aegean (NE Mediterranean) during the last 1500 years. *Quaternary*
876 *Science Reviews* 136, 209–228. doi:10.1016/j.quascirev.2016.01.009

- 877 Gotelli, N.J., Graves, G.R., 1996. Null models in ecology. *Ecology* 14, 368.
878 doi:10.1007/BF01199989
- 879 Griggs, C., DeGaetano, A., Kuniholm, P.I., Newton, M., 2007. A regional high-frequency
880 reconstruction of May–June precipitation in the north Aegean from oak tree rings, A.D.
881 1089–1989. *International Journal of Climatology* 27, 1075–1089. doi:10.1002/joc.1459 A
- 882 Grimm, E.C., 1992. TILIA and Tilia-Graph Software, Version 2.0. [WWW Document].
- 883 Heck, K.L.J., Belle, G. Van, Simberloff, D., 1975. Explicit Calculation of the Rarefaction
884 Diversity Measurement and the Determination of Sufficient Sample Size. *Ecology* 56,
885 1459–1461. doi:10.2307/1934716
- 886 Horvat, I., Glavac, V., Ellenberg, H., 1974. *Vegetation of Southeast-Europe*. Gustav Fischer
887 Verlag, Stuttgart.
- 888 Hughes, P.D., 2010. Little Ice Age glaciers in the Balkans: low altitude glaciation enabled by
889 cooler temperatures and local topoclimatic controls. *Earth Surface Processes and Landforms*
890 241, 229–241. doi:10.1002/esp.1916
- 891 Izdebski, A., Koloch, G., Słoczynski, T., 2015. Exploring Byzantine and Ottoman economic
892 history with the use of palynological data : a quantitative approach. *Jahrbuch der*
893 *österreichischen Byzantinistik* 31, 277–289.
- 894 Jones, P.D., Briffa, K.R., Barnett, T.P., Tett, S.F.B., 1998. High-resolution palaeoclimatic
895 records for the last millennium: interpretation, integration and comparison with General
896 Circulation Model control-run temperatures. *The Holocene* 8, 455–471.
897 doi:10.1191/095968398667194956
- 898 Kaplan, J.O., Krumhardt, K.M., Zimmerman, N., 2009. The prehistoric and preindustrial
899 deforestation of Europe. *Quaternary Science Reviews* 28, 3016–3034.

- 900 doi:10.1016/j.quascirev.2009.09.028.
- 901 Karadzić, B., Jarić, S., Pavlović, P., Mitrović, M., 2015. Aquatic and Wetland Vegetation Along
902 the Sava River. In: Milačić, R., Ščančar, J., Punović, M. (Eds.), *The Sava River*. Springer,
903 Heidelberg New York Dordrecht London, pp. 249–316. doi:10.1007/978-3-662-44034-6
- 904 Kern, Z., Németh, A., Horoszné Gulyás, M., Popa, I., Levanič, T., Hatvani, I.G., 2016. Natural
905 proxy records of temperature- and hydroclimate variability with annual resolution from the
906 Northern Balkan–Carpathian region for the past millennium – Review & recalibration.
907 *Quaternary International* 415, 109–125. doi:10.1016/j.quaint.2016.01.012
- 908 Kitnaes, K.S., Plavac, I., Posavec Vukelic, V., Rodić Baranović, P., Trenc, N., Topić, R., 2009.
909 *Protection of Biodiversity of the Sava River Basin Floodplains*.
- 910 Kouli, K., 2012. Vegetation development and human activities in Attiki (SE Greece) during the
911 last 5,000 years. *Vegetation History and Archaeobotany* 21, 267–278. doi:10.1007/s00334-
912 011-0336-9
- 913 Koutsodendris, A., Brauer, A., Reed, J.M., Plessen, B., Friedrich, O., Hennrich, B., Zacharias, I.,
914 Pross, J., 2017. Climate variability in SE Europe since 1450 AD based on a varved sediment
915 record from Etoliko Lagoon (Western Greece). *Quaternary Science Reviews* 159, 63–76.
916 doi:10.1016/j.quascirev.2017.01.010
- 917 Kulkarni, C., Peteet, D.M., Boger, R., Heusser, L.E., 2016. Exploring the role of humans and
918 climate over the Balkan landscape: 500 years of vegetational history of Serbia. *Quaternary
919 Science Reviews* 144, 83–94. doi:10.1016/j.quascirev.2016.05.021
- 920 Kuneš, P., Svobodová-Svitavská, H., Kolář, J., Hajnalová, M., Abraham, V., Macek, M., Tkáč,
921 P., Szabó, P., 2015. The origin of grasslands in the temperate forest zone of east-central
922 Europe: long-term legacy of climate and human impact. *Quaternary Science Reviews* 116,

- 923 15–27. doi:10.1016/j.quascirev.2015.03.014
- 924 Lamb, H.H., 1965. The early Medieval Warm Epoch and its sequel. *Palaeogeography,*
925 *Palaeoclimatology, Palaeoecology* 1, 13–37.
- 926 Leng, M.J., Wagner, B., Boehm, A., Panagiotopoulos, K., Vane, C.H., Snelling, A., Haidon, C.,
927 Woodley, E., Vogel, H., Zanchetta, G., Baneschi, I., 2013. Understanding past climatic and
928 hydrological variability in the mediterranean from Lake Prespa sediment isotope and
929 geochemical record over the last glacial cycle. *Quaternary Science Reviews* 66, 123–136.
930 doi:10.1016/j.quascirev.2012.07.015
- 931 Ljungqvist, F.C., 2010. A regional approach to the medieval warm period and the little ice age.
932 *Climate Change and Variability* 1–26.
- 933 Luterbacher, J., Dietrich, D., Xoplaki, E., Grosjean, M., Wanner, H., 2004. European seasonal
934 and annual temperature variability, trends, and extremes since 1500. *Science* 303, 1499–
935 503. doi:10.1126/science.1093877
- 936 Luterbacher, J., García-Herrera, R., Allan, A.R., Alvarez-Castro, B.G., Benito, G., Booth, J.,
937 Büntgen, U., Colombaroli, D., Davis, B., Esper, J., Felis, T., Fleitmann, D., Frank, D.,
938 Gallego, D., Gonzalez-Rouco, F.J., Goosse, H., Kiefer, T., Macklin, M.G., Montagna, P.,
939 Newman, L., Power, M.J., Rath, V., Ribera, P., Roberts, N., Silenzi, S., Tinner, W., Valero-
940 Garces, B., Schrier, G. Van der, Vannièrè, B., Wanner, H., Werner, J.P., Willett, G.,
941 Xoplaki, E., Zerefos, C.S., Zorita, E., 2011. A review of 2000 years of paleoclimatic
942 evidence in the Mediterranean. In: Lionello, P. (Ed.), *The Climate of the Mediterranean*
943 *Region*. Elsevier Ltd, pp. 1–119.
- 944 Magyari, E.K., Chapman, J.C., Passmore, D.G., Allen, J.R.M., Huntley, J.P., Huntley, B., 2010.
945 Holocene persistence of wooded steppe in the Great Hungarian Plain. *Journal of*

- 946 Biogeography 37, 915–935. doi:10.1111/j.1365-2699.2009.02261.x
- 947 Mann, M.E., 2002. The Little Ice Age. *Encyclopedia of Global Environmental Change* 1, 504–
948 509.
- 949 Mann, M.E., Bradley, R.S., Hughes, M.K., 1999. Northern hemisphere temperatures during the
950 past millennium: Inferences, uncertainties, and limitations. *Geophysical Research Letters*
951 26, 759–762. doi:10.1016/S0968-0004(96)90128-0
- 952 Mann, M.E., Zhang, Z., Rutherford, S., Bradley, R.S., Hughes, M.K., Shindell, D., Ammann,
953 C.M., Faluvegi, G., Ni, F., Shindell, D., Ammann, C.M., Faluvegi, G., Ni, F., 2009. Global
954 signatures and dynamical origins of the Little Ice Age and Medieval Climate Anomaly.
955 *Science* 78, 1256–1260. doi:10.1126/science.1166349
- 956 Marinova, E., Tonkov, S., Bozilova, E., Vajsov, I., 2012. Holocene anthropogenic landscapes in
957 the Balkans: The palaeobotanical evidence from southwestern Bulgaria. *Vegetation History*
958 *and Archaeobotany* 21, 413–427. doi:10.1007/s00334-011-0345-8
- 959 Masson-Delmotte, V., Schulz, M., Abe-Ouchi, A., Beer, J., Ganopolski, A., Rouco, J.F.G.,
960 Jansen, E., Lambeck, K., Luterbacher, J., Naish, T., Osborn, T., Otto-Bliesner, B., Quinn,
961 T., Ramesh, R., Rojas, M., Shao, X., Timmermann, A., 2013. Information from
962 Paleoclimate Archives. In: Stocker, T.F., Qin, D., Plattner, G.-K., Tignor, M., Allen, S.K.,
963 Boschung, J., Nauels, A., Xia, Y., Bex, V., Midgley, P.M. (Eds.), *Climate Change 2013 -*
964 *The Physical Science Basis . Contribution of Working Group I to the Fifth Assessment*
965 *Report of the Intergovernmental Panel on Climate Change*. Cambridge, UK and New York,
966 NY, USA. doi:10.1017/CBO9781107415324.013
- 967 Matthews, J.A., Briffa, K.R., 2005. the “Little Ice Age”: Re-Evaluation of an Evolving Concept.
968 *Geografiska Annaler: Series A, Physical Geography* 87, 17–36. doi:10.1111/j.0435-

- 969 3676.2005.00242.x
- 970 Mazier, F., Gaillard, M.J., Kuneš, P., Sugita, S., Trondman, A.K., Broström, A., 2012. Testing
971 the effect of site selection and parameter setting on REVEALS-model estimates of plant
972 abundance using the Czech Quaternary Palynological Database. *Review of Palaeobotany
973 and Palynology* 187, 38–49. doi:10.1016/j.revpalbo.2012.07.017
- 974 McEvedy, C., Jones, R., 1978. *Atlas of World Population History*. Penguin Books Ltd., London.
- 975 Meltsov, V., Poska, A., Odgaard, B. V., Sammul, M., Kull, T., 2011. Palynological richness and
976 pollen sample evenness in relation to local floristic diversity in southern Estonia. *Review of
977 Palaeobotany and Palynology* 166, 344–351. doi:10.1016/j.revpalbo.2011.06.008
- 978 Mercuri, A.M., Sadori, L., 2014. *Mediterranean Culture and Climatic Change: Past Patterns and
979 Future Trends*. In: Goffredo, S., Dubinsky, Z. (Eds.), *The Mediterranean Sea: Its History
980 and Present Challenges*. Springer Science+Business Media, Dordrecht, Netherlands, pp.
981 507–527. doi:10.1007/978-94-007-6704-1
- 982 Mercuri, A.M., Bandini Mazzanti, M., Florenzano, A., Montecchi, M.C., Rattighieri, E., 2013.
983 *Olea, Juglans and Castanea: The OJC group as pollen evidence of the development of
984 human-induced environments in the Italian peninsula*. *Quaternary International* 303, 24–42.
985 doi:10.1016/j.quaint.2013.01.005
- 986 Milačič, R., Ščančar, J., Paunović, M., 2014. *The Sava River, The Handbo.* ed. Springer,
987 Heidelberg New York Dordrecht London. doi:10.1007/978-3-662-44034-6
- 988 Milojević, B., 1954. *Geografski lik Srbije u vreme Prvog srpskog ustanka 1804–1813*
989 [Geographical Features of Serbia in the time of the First Uprising 1804–1813]. Srpsko
990 geografsko društvo, Belgrade, Serbia.
- 991 Mitchell, B.R., Kicosev, S., 1997. *A brief population history of the Vojvodina 1683-1718*.

- 992 Geographica Pannonica 12, 18–21.
- 993 Moore, P.D., Webb, J.A., Collison, M.E., 1991. Pollen analysis. Blackwell Scientific
994 Publications, Oxford, UK.
- 995 Mrgić, J., 2011. Wine or raki - The interplay of climate and society in early modern Ottoman
996 Bosnia. *Environment and History* 17, 613–637. doi:10.3197/096734011X13150366551652
- 997 Nicault, A., Alleaume, S., Brewer, S., Carrer, M., Nola, P., Guttierrez, E., Edouard, J.L., Urbinati,
998 C., Guiot, J., 2008. Mediterranean drought fluctuation during the last 500 years based on
999 tree-ring data. *Climate Dynamics* 31, 227–245. doi:10.1007/s00382-008-0404-8
- 1000 Nielsen, A.B., Giesecke, T., Theuerkauf, M., Feeser, I., Behre, K.E., Beug, H., Chen, S.H.,
1001 Christiansen, J., Dorfler, W., Endtmann, E., Jahns, S., Klerk, P. de, Kuhl, N., Latalowa, M.,
1002 Odgaard, B.V., Rasmussen, P., Stockholm, J.R., Voigt, R., Wiethold, J., Wolters, S., 2012.
1003 Quantitative reconstructions of changes in regional openness in north-central Europe reveal
1004 new insights into old questions. *Quaternary Science Reviews* 47, 131–149.
1005 doi:10.1016/j.quascirev.2012.05.011
- 1006 PAGES Hydro2k Consortium, 2017. Comparing proxy and model estimates of hydroclimate
1007 variability and change over the Common Era. *Climate of the Past* 13, 1851–1900.
- 1008 Palairet, M.R., 1997. *The Balkan Economies c. 1800-1914. Evolution Without Development.*
1009 Cambridge University Press.
- 1010 Panagiotopoulos, K., Aufgebauer, A., Schäbitz, F., Wagner, B., 2013. Vegetation and climate
1011 history of the Lake Prespa region since the Lateglacial. *Quaternary International* 293, 157–
1012 169. doi:http://dx.doi.org/10.1016/j.quaint.2012.05.048
- 1013 Peterken, G.F., Mountford, E.P., 1996. Effects of drought on beech in Lady Park Wood, an
1014 unmanaged mixed deciduous woodland. *Forestry* 69, 125–136.

- 1015 doi:10.1093/forestry/69.2.125
- 1016 Poljanšek, S., Ceglar, A., Levanič, T., 2013. Long-term summer sunshine/moisture stress
1017 reconstruction from tree-ring widths from Bosnia and Herzegovina. *Climate of the Past* 9,
1018 27–40. doi:10.5194/cp-9-27-2013
- 1019 Popa, I., Bouriaud, O., 2014. Reconstruction of summer temperatures in Eastern Carpathian
1020 Mountains (Rodna Mts, Romania) back to AD 1460 from tree-rings. *International Journal of*
1021 *Climatology* 34, 871–880. doi:10.1002/joc.3730
- 1022 Popa, I., Kern, Z., 2009. Long-term summer temperature reconstruction inferred from tree-ring
1023 records from the Eastern Carpathians. *Climate Dynamics* 32, 1107–1117.
1024 doi:10.1007/s00382-008-0439-x
- 1025 Popović, M., 2012. Spatbyzantinische siedhingen und wlachische transhumanz in den fhisstalem
1026 der strumica und kriva laka-vica, Siklosteuropaische Romania: Siedhings-
1027 /Migrationsgeschiclite und Sprachtypologie. *Romanistisches Kolloquium XXV. Tübinger*
1028 *Beitrage Zur Linguistik*, Narr, Tübingen.
- 1029 Purgstall, B.J.V.H., 1983. *Ottoman state history*, Vol 1–7. Translator: Vecdi Burun, Ucdal
1030 Publishing, Istanbul (in Turkish).
- 1031 Qiriazzi, P., Sala, S., 2000. Environmental problems of Albania. In: Buchroithner, M., F. (Ed.),
1032 *Remote Sensing for Environmental Data in Albania: A Strategy for Integrated Management*.
1033 Kluwer, Dordrecht, pp. 13–30.
- 1034 R Core Team, 2014. *R: a language and environment for statistical computing*.
- 1035 Radović, I., Kozomara, M. (Eds.), 2011. *Biodiversity strategy of the Republic of Serbia for the*
1036 *period 2011–2018*. Ministry of Environment and Spatial Planning, Republic of Serbia,
1037 Belgrade.

- 1038 Rakonjac, L., Nevenic, R., 2012. Reforestation in Serbia: Potential Vegetation Type and
1039 Selection in Afforestation Central Serbia. LAP Lambert Academic Publishing, Saarbrucken,
1040 Germany.
- 1041 Reale, O., Shukla, J., 2000. Modeling the effects of vegetation on Mediterranean climate during
1042 the Roman Classical Period: Part II. Model simulation. *Global and Planetary Change* 25,
1043 185–214. doi:10.1016/S0921-8181(00)00003-5
- 1044 Reille, M., 1999. Pollen et Spores d' Europe et d' Afrique du nord. Laboratoire de Botanique
1045 Historique et Palynologie, Marseille.
- 1046 Reimer, P., Bard, E., Bayliss, A., 2013. IntCal13 and Marine13 Radiocarbon Age Calibration
1047 Curves 0–50,000 Years cal BP. *Radiocarbon* 55, 1869–1887.
1048 doi:10.2458/azu_js_rc.55.16947
- 1049 Renberg, I., Bindler, R., Brannvall, M.L., 2001. Using the historical atmospheric lead-deposition
1050 record as a chronological marker in sediment deposits in Europe. *Holocene* 11, 511–516.
1051 doi:10.1191/095968301680223468
- 1052 RHMSS, 2015. Basic climate characteristics for the territory of Serbia (standard normal period
1053 1961-1990) [WWW Document]. Republic Hydrometeorological Service of Serbia. URL
1054 http://www.hidmet.gov.rs/eng/meteorologija/klimatologija_srbije.php (accessed 4.7.15).
- 1055 Roberts, N., Moreno, A., Valero-Garcés, B.L., Corella, J.P., Jones, M., Allcock, S., Woodbridge,
1056 J., Morellón, M., Luterbacher, J., Xoplaki, E., Türkeş, M., 2012. Palaeolimnological
1057 evidence for an east-west climate see-saw in the Mediterranean since AD 900. *Global and*
1058 *Planetary Change* 84–85, 23–34. doi:10.1016/j.gloplacha.2011.11.002
- 1059 Schnitchen, C., Charman, D.J., Magyari, E., Braun, M., Grigorszky, I., Tóthmérész, B., Molnár,
1060 M., Szántó, Z., 2006. Reconstructing hydrological variability from testate amoebae analysis

- 1061 in Carpathian peatlands. *Journal of Paleolimnology* 36, 1–17. doi:10.1007/s10933-006-
1062 0001-y
- 1063 Seim, A., Buntgen, U., Fonti, P., Haska, H., Herzig, F., Tegel, W., Trouet, V., Treydte, K., 2012.
1064 Climate sensitivity of a millennium-long pine chronology from Albania. *Climate Research*
1065 51, 217–228. doi:10.3354/cr01076
- 1066 Sekulić, G., Dimović, D., Jović, Z., Todorović, N., 2012. *Climate Vulnerability Assessment -*
1067 *Serbia*. WWF (World Wide Fund for Nature), Environmental Improvement Centre,
1068 Belgrade, Serbia.
- 1069 Stockmarr, J., 1971. Tablets with spores used in absolute pollen analysis. *Pollen et Spores* 13,
1070 615–621.
- 1071 Stoianovich, T., 1992. *Balkan Worlds: The First and Last Europe*. Routledge.
- 1072 Sugita, S., 2007. Theory of quantitative reconstruction of vegetation I: pollen from large sites
1073 REVEALS regional vegetation composition. *The Holocene* 17, 229–241.
1074 doi:10.1177/0959683607075837
- 1075 Theuerkauf, M., Couwenberg, J., Kuparinen, A., Liebscher, V., 2016. A matter of dispersal:
1076 REVEALSinR introduces state-of-the-art dispersal models to quantitative vegetation
1077 reconstruction. *Vegetation History and Archaeobotany* 25, 541–553. doi:10.1007/s00334-
1078 016-0572-0
- 1079 Thienemann, M., Masi, A., Kusch, S., Sadori, L., John, S., Francke, A., Wagner, B., Rethemeyer,
1080 J., 2017. Organic geochemical and palynological evidence for Holocene natural and
1081 anthropogenic environmental change at Lake Dojran (Macedonia/Greece). *The Holocene*
1082 959683616683261. doi:10.1177/0959683616683261
- 1083 Toljić, M., Matenco, L., Ducea, M.N., Stojadinović, U., Milivojević, J., Derić, N., 2013. The

- 1084 evolution of a key segment in the Europe-Adria collision: The Fruška Gora of northern Serbia.
1085 *Global and Planetary Change* 103, 39–62. doi:10.1016/j.gloplacha.2012.10.009
- 1086 Tonkov, S., 2003. Holocene palaeovegetation of the Northwestern Pirin Mountains (Bulgaria) as
1087 reconstructed from pollen analysis. *Review of Palaeobotany and Palynology* 124, 51–61.
1088 doi:10.1016/S0034-6667(02)00247-6
- 1089 Touchan, R., Xoplaki, E., Funkhouser, G., Luterbacher, J., Hughes, M.K., Erkan, N., Akkemik,
1090 Ü., Stephan, J., 2005. Reconstructions of spring/summer precipitation for the Eastern
1091 Mediterranean from tree-ring widths and its connection to large-scale atmospheric
1092 circulation. *Climate Dynamics* 25, 75–98. doi:10.1007/s00382-005-0016-5
- 1093 Welden, A. Van, Beck, C., Reyss, J.L., Bushati, S., Koci, R., Jouanne, F., Mugnier, J.L., 2008.
1094 The last 500 years of sedimentation in Shkodra Lake (Albania/Montenegro):
1095 Paleoenvironmental evolution and potential for paleoseismicity studies. *Journal of*
1096 *Paleolimnology* 40, 619–633. doi:10.1007/s10933-007-9186-y
- 1097 White, S.A., 2006. Climate changes and crisis in Ottoman Turkey and the Balkans, 1590–1710.
1098 In: *Climate Change and the Middle East: Past, Present*. Istanbul Technical University,
1099 Turkey., pp. 391–429.
- 1100 White, S.A., 2011. *The climate of the rebellion in the Early Modern Ottoman empire*. Cambridge
1101 University Press, Cambridge, UK.
- 1102 Whitlock, C., Larsen, C., 2001. Charcoal as a Fire Proxy. In: Smol, J.S., Birks, H.J.B., Last,
1103 W.M. (Eds.), *Tracking Environmental Change Using Lake Sediments*. Kluwer Academic
1104 Publishers, Dordrecht, The Netherlands, pp. 75–97.
- 1105 Widlok, T., Aufgebauer, A., Bradtmöller, M., Dikau, R., Hoffmann, T., Kretschmer, I.,
1106 Panagiotopoulos, K., Pastoors, A., Peters, R., Schäbitz, F., Schlummer, M., Solich, M.,

- 1107 Wagner, B., Weniger, G.C., Zimmermann, A., 2012. Towards a theoretical framework for
1108 analyzing integrated socio-environmental systems. *Quaternary International* 274, 259–272.
1109 doi:10.1016/j.quaint.2012.01.020
- 1110 Willis, K.J., Braun, M., Bennett, K.D., 1998. Prehistoric land degradation in Hungary: who, how
1111 and why? *Antiquity* 72, 101–111.
- 1112 Wright, H.E., Mann, D.H., Glaser, P.H., 1984. Piston corers for peat and lake sediments.
1113 *Ecology* 65, 657–659.
- 1114 Xoplaki, E., Maheras, P., Luterbacher, J., 2001. Variability of climate in Meridional Balkans
1115 during the periods 1675–1715 and 1780–1830 and its impact on human life. *Climatic*
1116 *Change* 48, 581–615.
- 1117 Zanchetta, G., Welden, A. van, Baneschi, I., Drysdale, R., Sadori, L., Roberts, N., Giardini, M.,
1118 Beck, C., Pascucci, V., Sulpizio, R., Sapienza, L., 2012. Multiproxy record for the last 4500
1119 years from Lake Shkodra (Albania/Montenegro). *Journal of Quaternary Science* 27, 780–
1120 789. doi:10.1002/jqs.2563
- 1121 Zerefos, C.S., Repapis, C., Giannakopoulos, C., Kapsomenakis, J., Papanikolaou, D.,
1122 Papanikolaou, M., Poulos, S., Vrekoussis, M., Philandras, C., Tselioudis, G., Gerasopoulos,
1123 E., Douvis, C., Diakakis, M., Nastos, P., Hadjinicolaou, P., Xoplaki, E., Luterbacher, J.,
1124 Zanis, P., Tzedakis, P.C., Founda, D., Eleftheratos, K., Repapis, K., 2011. The climate of
1125 the Eastern Mediterranean and Greece: past, present and future. In: *The Environmental,*
1126 *Economic and Social Impacts of Climate Change in Greece.* Bank of Greece, Athens, pp. 1–
1127 126.

1128 **Figure Captions**

1129 **Fig. 1 a** Quaternary-Holocene pollen records (black dots) from the Balkans (green highlighted
1130 region) and surrounding regions (Data source: <http://www.europeanpollendatabase.net/data/>;
1131 Andric, 2016; Andric and Willis, 2003; Chapman et al., 2009; Finsinger et al., 2017; Gardner
1132 and Willis, 1999; Willis et al., 1998). The location of Serbia (purple) is shown. **b** Location of the
1133 Sava Basin (dotted region) within Serbia. The black dot shows the location of the only high-
1134 resolution last millennium pollen record from Serbia (Kulkarni et al., 2016). **c** Google Image of
1135 the study area showing the location of the Sava River and the Zivaca oxbow lake under
1136 investigation. (Data source: www.googleEarth.com). The star shows the location of the coring
1137 site.

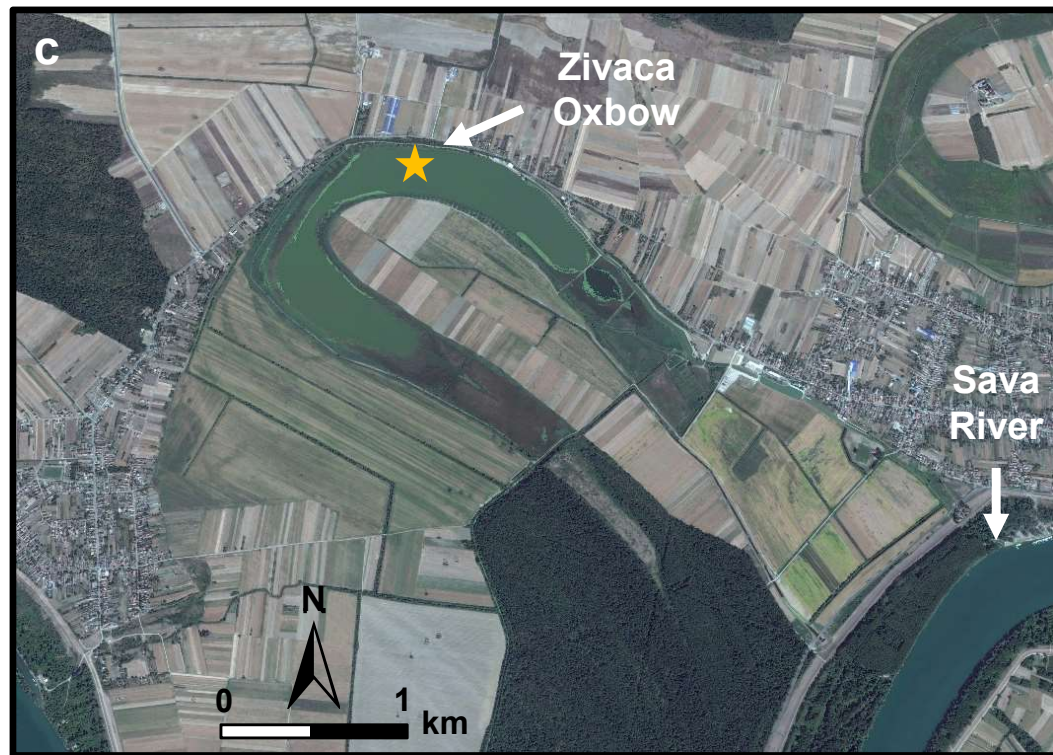
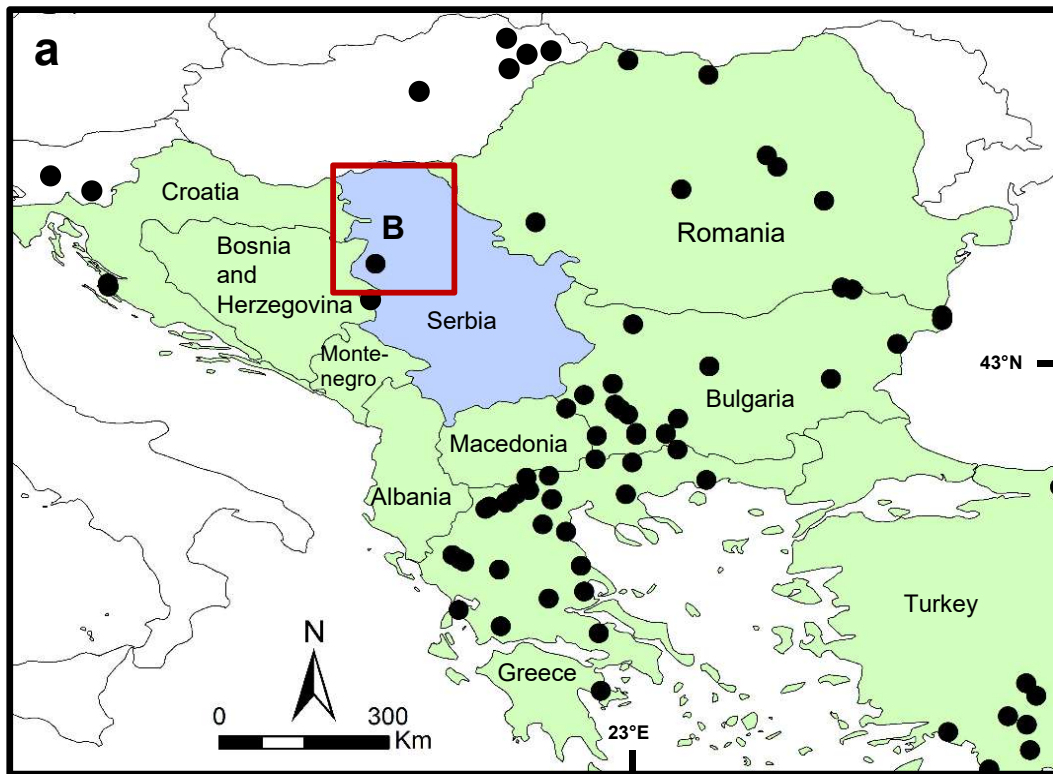
1138
1139 **Fig. 2 a** Lithology and the changes in atmospheric lead (expressed as a Pb/Ti ratio) across ZO
1140 core. The consistent decline in Pb/Ti is shown with a red arrow, which provides a chronological
1141 marker in building the age-depth model (See Supplementary Content). **b** Age-depth model
1142 constructed in Bacon 2.2 where the mean accumulation of 2 yr/cm was used as a priori
1143 information (Blaauw and Christen, 2011). Blue symbols are the age estimates with associated
1144 uncertainties and the solid red curve shows the weighted mean based age for each depth (Blaauw
1145 and Christen, 2013).

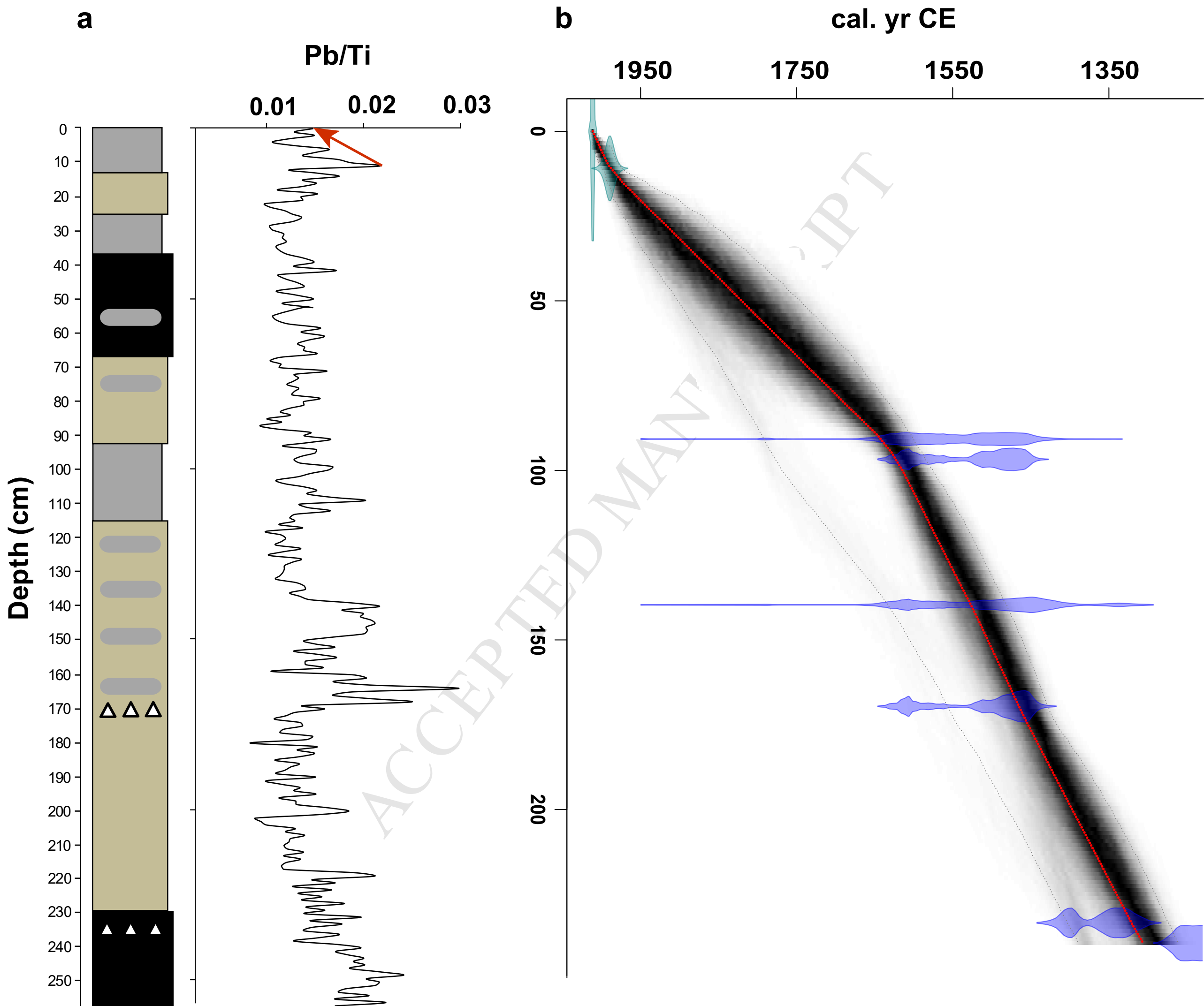
1146
1147 **Fig. 3** Lithology, inorganic and organic content (%), potassium (K), titanium (Ti) and calcium
1148 (Ca) counts (ppm) for ZO core. The dotted lines represent the respective pollen assemblage
1149 zones; refer to description and Figs. 4-5 for details.

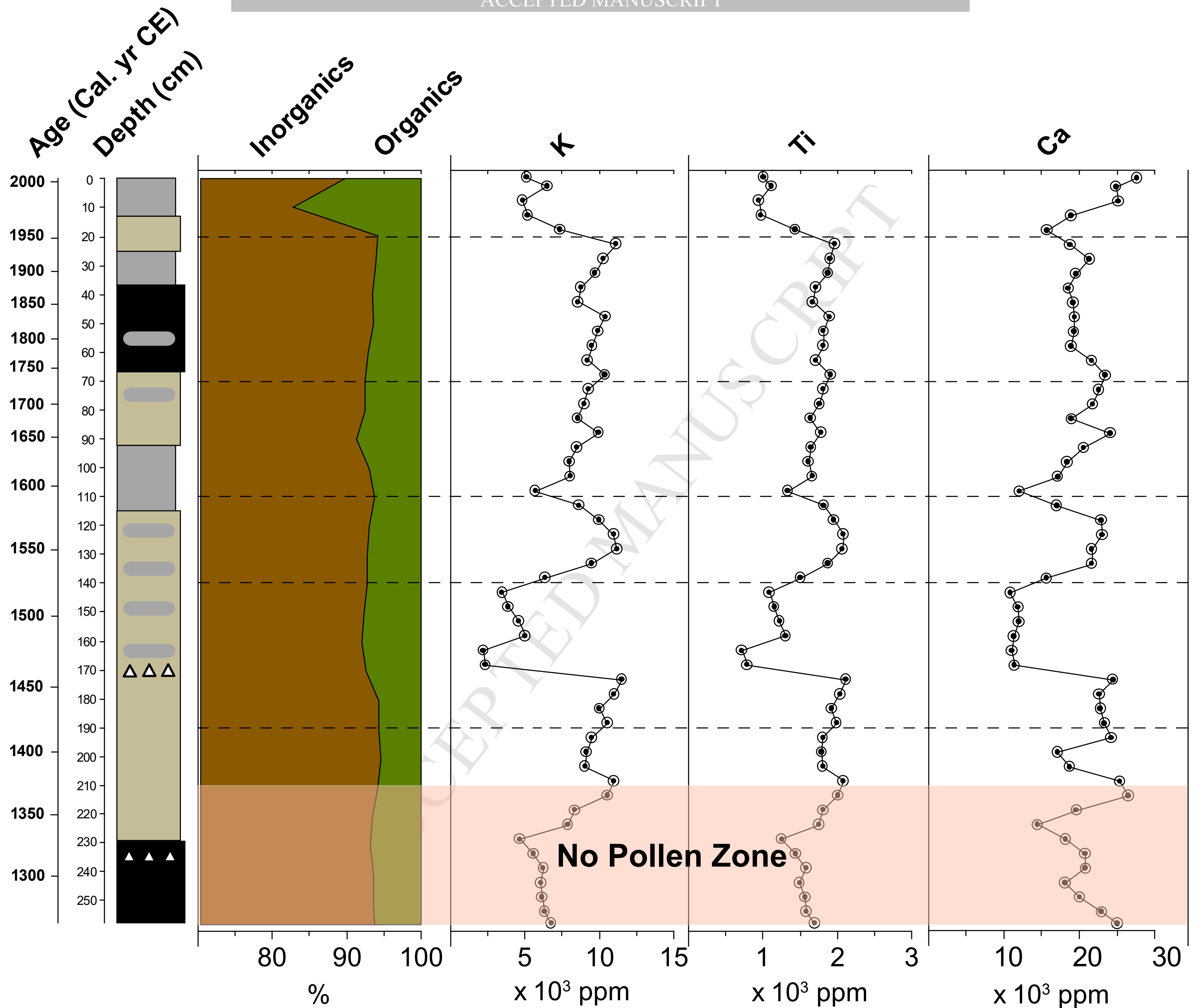
1150

1151 **Fig. 4** Estimated regional vegetation cover based on the REVEALS model (colored silhouettes)
1152 and pollen percentages (black lines) for 27 taxa in the Sava Region. Taxa groups are also
1153 presented. Horizontal lines separate major vegetation zones analogous to CONISS-based pollen
1154 assemblage zones (See Supplementary Fig. S1). The blue highlighted region shows the accepted
1155 extent of the Little Ice Age (LIA; 1450-1850 CE).

1156
1157 **Fig. 5** Composite diagram of the ZO sequence, Sava Region: REVEALS-based forested, open
1158 and crop land fractions, palynological richness, pollen and charcoal influxes, and geochemical
1159 indicators. The historic timeline is provided with major socio-political events including major
1160 wars (gray boxes). The blue highlighted region shows the accepted extent of the Little Ice Age
1161 (LIA; 1450-1850 CE).







Shells



Clay



Silty Clay



Silt

